

## Quantum breakdown of superconductivity in low-dimensional materials

Sacépé, Benjamin; Feigel'man, Mikhail; Klapwijk, Teunis M.

**DOI**

[10.1038/s41567-020-0905-x](https://doi.org/10.1038/s41567-020-0905-x)

**Publication date**

2020

**Document Version**

Accepted author manuscript

**Published in**

Nature Physics

**Citation (APA)**

Sacépé, B., Feigel'man, M., & Klapwijk, T. M. (2020). Quantum breakdown of superconductivity in low-dimensional materials. *Nature Physics*, *16*(7), 734-746. <https://doi.org/10.1038/s41567-020-0905-x>

**Important note**

To cite this publication, please use the final published version (if applicable). Please check the document version above.

**Copyright**

Other than for strictly personal use, it is not permitted to download, forward or distribute the text or part of it, without the consent of the author(s) and/or copyright holder(s), unless the work is under an open content license such as Creative Commons.

**Takedown policy**

Please contact us and provide details if you believe this document breaches copyrights. We will remove access to the work immediately and investigate your claim.



# Quantum breakdown of superconductivity in low-dimensional materials

Benjamin Sacépé<sup>1</sup>✉, Mikhail Feigel'man<sup>2,3</sup> and Teunis M. Klapwijk<sup>4,5,6</sup>

**In order to understand the emergence of superconductivity it is useful to study the reverse process and identify the various pathways that lead to its destruction. One way is to increase the amount of disorder, as this leads to an increase in Coulomb repulsion that overpowers the attractive interaction responsible for Cooper pair formation. A second pathway—applicable to uniformly disordered materials—is to utilise the competition between superconductivity and Anderson localisation, as this leads to electronic granularity in which phase and amplitude fluctuations of the superconducting order parameter play a role. Finally, a third pathway is to construct an array of superconducting islands coupled by some form of proximity effect that leads from a superconducting state to a state with finite resistivity, which appears like a metallic groundstate. This Review Article summarizes recent progress in understanding of these different pathways, including experiments in low dimensional materials and application in superconducting quantum devices.**

In parallel to the continuous discovery of new superconducting materials, a different research strategy can be followed that concentrates on the destruction of superconductivity in a given materials system. Instead of changing the chemical composition of the material, the approach is to change a parameter intrinsic to the material such as electron density, disorder, or dimensionality, and so drive a transition from a superconducting state to another state, which is often found to be an insulator or a metal. It is experimentally unavoidable that this transition must be monitored at finite temperature ( $T$ ), but the physics is focused on the transition that is expected to occur at zero temperature reflecting a transition from one ground state to another, a quantum phase transition<sup>1</sup>. This quantum phase transition has—with some theoretical bias—traditionally been called a superconductor–insulator transition<sup>2</sup>, and has been studied in numerous experimental configurations and materials, encompassing amorphous thin films, granular superconductors, nanowires, gate-tunable superconducting oxide interfaces, aluminum-based Josephson junction arrays, proximitised metals and semiconductors<sup>3,4,5,6</sup> or two-dimensional (2D) crystalline superconductors.

In the last decade, the detailed study of the transition has revealed many surprises that have drastically changed our understanding of conventional superconductivity and has shown some links to phenomena observed in high temperature cuprate superconductors. These new developments are the focus of this Review. To remove interpretative bias in the terminology we use in throughout, we adopt a more neutral term ‘quantum breakdown of superconductivity’ (QBS) instead of the commonly used term ‘superconductor–insulator transition’ (SIT). We restrict use of the term SIT to situations involving a transition to an insulating state and use the phrase ‘superconductor–metal transition’ (SMT) if it transitions into a metal-like state. As we will see, even these ‘insulator’ and ‘metal’ states can also be based on ingredients related to the superconducting state, without showing zero resistance.

## Main paradigms

Various means can be employed to study experimentally the evolution of superconductivity towards breakdown. Some obvious ones are the application of an external magnetic field ( $B$ ) or a d.c.

current, which lead to the transition to resistive superconducting states. Suitable materials can be created by either increasing disorder, changing the carrier density by field-effect gating or by using a lower effective dimensionality in thin-film, nanowire geometries or single-atom-thick layers. Understanding how the evolution of the superconducting order parameter  $\Psi = \Delta e^{i\phi}$  correlates with the suppression of the zero-resistance state is the primary question that provides insight on several fundamental concepts and paradigms of condensed matter physics.

The first key paradigm concerns the complex nature of the superconducting order parameter. The suppression of superconductivity can follow two main paths<sup>3</sup>, either a suppression of the amplitude  $\Delta$  or a loss of the stiffness of the phase  $\phi$ . The former involves the interaction between the electrons that sets the strength of the attractive interaction leading to Cooper pairing, and which may, if pushed from attractive to repulsive, restore the normal state<sup>4,5</sup>. The second one yields a less intuitive mechanism in which Cooper pairing remains and resistive properties emerge because the macroscopic phase loses long-range order and varies in time<sup>6</sup>. These two antagonistic mechanisms that both result in the destruction of superconductivity have been dubbed the fermionic and bosonic scenarios. Both yield resistive states, terminating the zero-resistance superconductivity, but are made from very different charge carriers, one formed of fermionic single electrons and the other of incoherent bosonic Cooper pairs.

Another important aspect to grasp is the effective dimensionality of the system. For single-electron coherence the relevant comparison is between the inelastic length and the thickness of a thin film or the width of a nanowire. However, for a superconductor the superconducting coherence length  $\xi$  is the scale to compare with the sample dimensions. Superconductivity is quasi-2D when one of the sample dimensions is smaller than  $\xi$ , and quasi-1D when two of them are. This reduced dimensionality has major consequences for the superconducting state<sup>7</sup>: it enhances fluctuations and generates topological defects—vortices in 2D or phase slips in 1D—that drastically modify the transport properties and eventually suppress the phase stiffness through a Berezinskii–Kosterlitz–Thouless transition or through 1D (quantum) phase slips.

<sup>1</sup>Univ. Grenoble Alpes, CNRS, Grenoble INP, Institut Néel, Grenoble, France. <sup>2</sup>L.D. Landau Institute for Theoretical Physics, Chernogolovka, Russia. <sup>3</sup>Skolkovo Institute for Science and Technology, Moscow, Russia. <sup>4</sup>Kavli Institute of Nanoscience, Delft University of Technology, Delft, The Netherlands. <sup>5</sup>Institute for Topological materials, Julius Maximilian University of Würzburg, Würzburg, Germany. <sup>6</sup>Physics Department, Moscow State University of Education, Moscow, Russia. ✉e-mail: [benjamin.sacepe@neel.cnrs.fr](mailto:benjamin.sacepe@neel.cnrs.fr)

64 Last but not least, disorder is an unavoidable ingredient that has  
 65 deep consequences in limiting electron transport in general and  
 66 which contrasts sharply with the zero-resistance property of super-  
 67 conductivity. Although disorder is at first sight incompatible with  
 68 superconductivity, experiments and theory show that supercon-  
 69 ductivity can develop in systems in which the single electrons are  
 70 localized, leading to an insulating state in the  $T = 0$  limit. If Cooper  
 71 pairing can develop with localized single-electron states, then the  
 72 natural question to ask is whether one may observe localization of  
 73 Cooper pairs. In the past decade, a large body of work has demon-  
 74 strated that this type of localization occurs in some amorphous  
 75 superconductors. Probing and understanding the properties of  
 76 insulating systems with localized Cooper pairs poses further chal-  
 77 lenges and intriguing questions.

78 These rather generic ingredients—reduced dimensions, disorder  
 79 and Coulombic inter-electron interactions—can be introduced  
 80 and controlled in many superconductors. Through decades of  
 81 research, primarily using magnetotransport and analysis of quantum  
 82 criticality, it has been found that the breakdown of supercon-  
 83 ductivity does not follow a universal path. Instead, there appears  
 84 to be almost as many QBSs as systems under study. This led to a  
 85 classification of various types of transition according to their  
 86 structural aspects, meaning whether they take place in granular  
 87 or homogeneously disordered (amorphous) systems; by the level  
 88 of charge carrier density; by their effective dimensionality; by the  
 89 type of weak link in Josephson junction arrays; or by the parameter  
 90 that drives the quantum phase transition. In this Review, we have  
 91 chosen to leave out a previously studied specific model system of  
 92 Josephson tunnel junction arrays with competing Josephson and  
 93 charging energies<sup>8</sup>.

94 Our review will highlight the new phenomena and concepts that  
 95 emerged recently and led the community to revisit several long-  
 96 standing paradigms in the field of the QBS. Experimentally, much  
 97 of the recent progress is due to the use of very low temperature  
 98 spectroscopy with local probes that unveils the emergent electronic  
 99 granularity in homogeneously disordered thin films and the exist-  
 100 ence of the pseudogap for preformed Cooper pairs. These discov-  
 101 eries led to the unexpected breakdown of the often-cited fermionic  
 102 and bosonic dichotomy and demand a new microscopic description  
 103 of superconductivity subject to strong disorder. Moreover, in a num-  
 104 ber of experimental systems the transition to the superconducting  
 105 state is found to be incomplete, that is, terminated by a metal-like  
 106 state down to the lowest accessible temperature<sup>9</sup>. This phenomenon  
 107 might be called a superconductor–metal transition, although the  
 108 origin of this vividly discussed<sup>10,11</sup> metallic state has not yet been  
 109 determined unambiguously. We also discuss how new gate-tunable  
 110 semiconductor and low-dimensional materials can be used to cou-  
 111 ple superconducting islands creating proximitized Josephson junc-  
 112 tion arrays, providing new insights into the QBS physics utilizing  
 113 insights from mesoscopic physics. Finally, we address how strong  
 114 disorder modifies the electrostatics near the QBS and how this  
 115 electrostatics can be utilised in hybrid quantum circuits.

### 117 **Amplitude- versus phase-driven transition**

118 Thin superconducting films have become the prototypical systems  
 119 to study the quantum breakdown of superconductivity. Due to their  
 120 quasi-2D nature, thermal and quantum fluctuations of the order  
 121 parameter  $\Psi = \Delta e^{i\phi}$  play a crucial role<sup>7,12</sup>. Thin films are furthermore  
 122 enhanced by disorder that reduces the superconducting coherence  
 123 length. At the same time, the diffusive motion of electrons impeded  
 124 by the reduced dimensionality tends to enhance the strength of  
 125 the Coulombic inter-electron interaction<sup>13</sup>. These two phenomena  
 126 generate two distinct pathways to QBS (Fig. 1): either a suppression  
 127 of the superconducting phase stiffness by quantum phase fluctua-  
 128 tions—the phase-driven pathway—or a Coulomb-assisted suppres-  
 129 sion of the Cooper-pair attraction—the amplitude pathway.

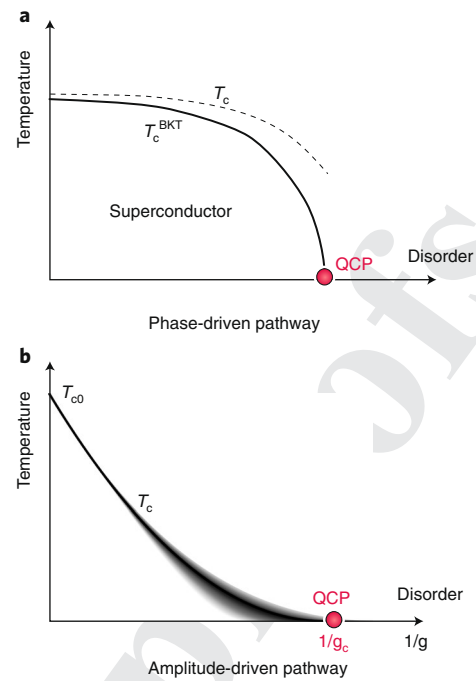


**Fig. 1 | The phase diagrams of 2D superconductors. a,**

Temperature-disorder phase diagram of 2D superconductors<sup>6</sup>. The transition to the superconducting state is defined by the critical temperature  $T_c$  at which the Cooper pairs preform. The superfluid stiffness, indicating superconductivity, develops at a lower temperature, below  $T_c^{\text{BKT}}$ , the critical temperature of the Berezinski-Kosterlitz-Thouless transition<sup>129,130</sup>. On increasing disorder,  $T_c$  is reduced by the Finkel'stein mechanism<sup>4,5</sup> illustrated in **b**. Similarly,  $T_c^{\text{BKT}}$  is suppressed faster due to the disorder-enhanced phase fluctuations, till a critical disorder that defines the quantum critical point (QCP). The existence of the two critical temperatures opens up a sizeable temperature regime for phase fluctuations<sup>12</sup> between  $T_c^{\text{BKT}}$  and  $T_c$ , which grows with increasing disorder. At the quantum critical point the superfluid stiffness vanishes, but without the destruction of the Cooper pairs. Without stipulating the nature of the state terminating superconductivity, metal or insulator, one recognizes that this scenario defines a prototypical continuous quantum phase transition<sup>1</sup>, driven by quantum fluctuations of the phase of the order parameter. **b**, Coulomb suppression of the critical temperature  $T_c$  as a function of disorder  $1/g$ , with  $g = h/e^2 R_{\square}$  according to Finkel'stein theory. The shaded grey area around the  $T_c$  line represents the fluctuations of the local critical temperature  $T_c(\mathbf{r})$  that develop and grow as  $\frac{\delta T_c}{T_c} \approx \frac{0.4}{g(g-g_c)}$  upon approaching the critical point  $1/g_c$  (ref. <sup>39</sup>). Notice that the disorder dependence of  $T_c$  takes the form drawn in **a** when plotted as a function of  $(1/g)$ , see for instance Figs. 4 and 5 in ref. <sup>131</sup>.

**Phase-driven pathway.** A seminal approach to the phase-driven QBS in thin-film superconductors was proposed by Matthew Fisher<sup>6</sup>, who developed the quantum critical scaling theory of the dirty boson model. It is a 2D model of hard-core, interacting bosons of charge  $2e$  (describing Cooper pairs) in a random potential. The fundamental concept of this work, which motivated considerable experimental activity on thin superconducting films, is the possibility that, when the magnetic field is increased at  $T = 0$ , the density of pinned vortices will increase and they can delocalize and undergo Bose condensation. A similar effect occurs for the vortex-anti-vortex phase when disorder is increased at  $B = 0$  (Fig. 1a). In analogy, this implies that the localisation of charge- $2e$  bosons must be mandatory for the condensation of the charge- $2e$  bosons in the superfluid phase. As a result, the QBS in this model is the competition between condensation of Cooper pairs and of vortices.

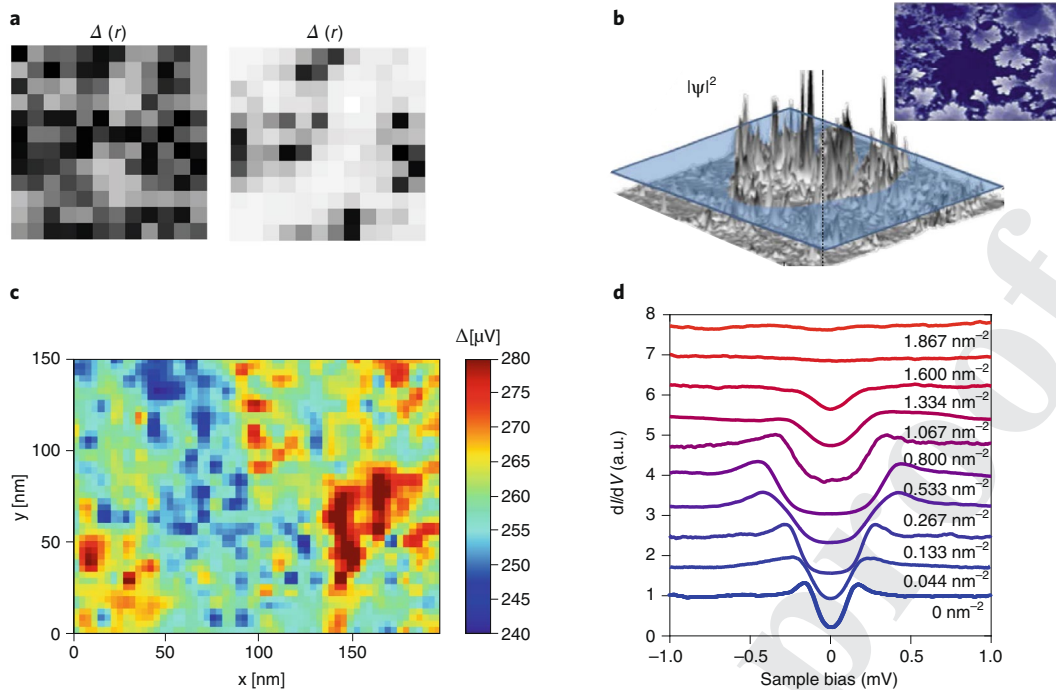


**Fig. 2 | Emergent superconducting granularity.** **a**, Spatial map of the pairing amplitude  $\Delta(r)$  obtained by numerical solution of the 2D disordered attractive Hubbard model<sup>36</sup> with a disorder level equal to the nearest-neighbor hopping (left) and to twice the nearest-neighbor hopping (right). Sites with darker gray-scale indicate larger  $\Delta(r)$ . **b**, Fractal wavefunction intensity  $|\psi|^2$  at the mobility edge for the Anderson problem. The fractal nature is readily seen in the inset that shows the spatial distribution of the wavefunction at the intensity indicated by the blue plane. The wavefunction occupies only a fraction of the available volume. **c**, Spatial map of the superconducting gap measured by scanning tunnelling spectroscopy on a TiN thin film<sup>26</sup> near the QBS ( $T_c \simeq 0.3T_{c0}$  and  $R_{\square} = 3.5k\Omega$  reached before the superconducting transition). Measurements were performed at 0.05 K. **d**, Tunneling conductance  $dI/dV$  measured by scanning tunnelling spectroscopy on an epitaxial monolayer of NbSe<sub>2</sub> covered by Si adatoms<sup>34</sup>. Each spectrum corresponds to a different surface density of adatoms, that is, different level of disorder. The superconducting gap evolves non-monotonously with the surface density of adatoms. Figure reproduced with permission from: **a**, ref. <sup>36</sup>, APS; **b**, V. Kravtsov; **c**, ref. <sup>26</sup>, APS; **d**, ref. <sup>34</sup>, Springer Nature Ltd.

Two major outcomes of this theory have laid the groundwork for decades of work on this specific theory for the QBS. First, the resistance at the quantum critical point is predicted to be metallic because the vortices and charges diffuse simultaneously and, if we assume a self-duality between the charges and vortices, it should reach the quantum resistance for charge  $2e$ ,  $h/(2e)^2$ . Secondly, the quantum scaling analysis led to a frequently used scaling dependence of the resistance around the quantum critical point:

$$R = \frac{h}{4e^2} \mathcal{F}(|\delta|/T^{1/z\nu}), \quad (1)$$

which relates the behaviour of the resistance to the critical exponents  $\nu$  and  $z$  of the diverging spatial and dynamical correlation lengths<sup>1</sup>, via the scaling functional  $\mathcal{F}$ . The variable  $\delta$  is defined as  $\delta = (X - X_c)/X_c$ , the distance to the critical point  $X_c$  for the tuning parameter  $X$ .

Experimentally, Hebard and Palaneen<sup>14</sup> were the first to uncover an intriguing crossing point in the magnetoresistance isotherms of amorphous InO (a:InO) films. The nearly  $T$ -independent resistance at the crossing point reached a value of  $0.7h/4e^2$  and was identified as the quantum critical point of the magnetic-field-driven SIT. Scaling analysis of the resistance data around it, taken at various  $T$ , were shown to collapse on a single functional, in accordance with equation (1), providing direct access to the critical exponents  $\nu$  and  $z$ . Another seminal work, conducted by Haviland et al.<sup>15</sup>, modified the disorder in quench-condensed amorphous bismuth films by tuning their thickness and discovered a QBS where the critical temperature is continuously reduced upon increasing sheet

resistance, reaching full suppression for a resistance of the order of  $h/(2e)^2$ .

These experimental findings, together with Fisher's theory, lent support to a phase-driven QBS scenario and stimulated a large body of experimental work to establish the universal character of the phase-driven QBS independently in various systems and materials. The studies carried out over the past three decades repeatedly confirmed the presence of a, sometimes approximate, crossing point in the magnetoresistance and reproduced with varying degrees of success the quantum scaling of the data. Unfortunately, the resulting collection of critical exponents extracted from scaling analysis covers a large range of values, ranging from  $z\nu = 0.6$  to 2.4. In order to reconcile this dispersion, different universality classes were invoked, for example for classical and quantum percolation<sup>16</sup> (see for example the reviews in refs. <sup>17,18</sup>). Even then, one finds a lack of universality for the critical exponents, often a limited range of temperature or field used for the scaling analysis, a non-perfect crossing point that sometimes transforms into multiple crossing points in different temperature ranges that is then interpreted as multiple quantum criticality<sup>19</sup>. All these observations have undermined the confidence in arguments based on the data scaling analysis. In retrospect, the quantum scaling analysis, which continues to be widely used as an indicator for quantum criticality, has become a mandatory figure for a phase-driven QBS while, at the same time, it has not been able to bring fruitful insight into the QBS physics, such as the understanding of the microscopic origin of the magnetoresistance crossing point.

Likewise, the critical resistance is found to cover a range from 1 to 30k $\Omega$ , although with variation from sample to sample around

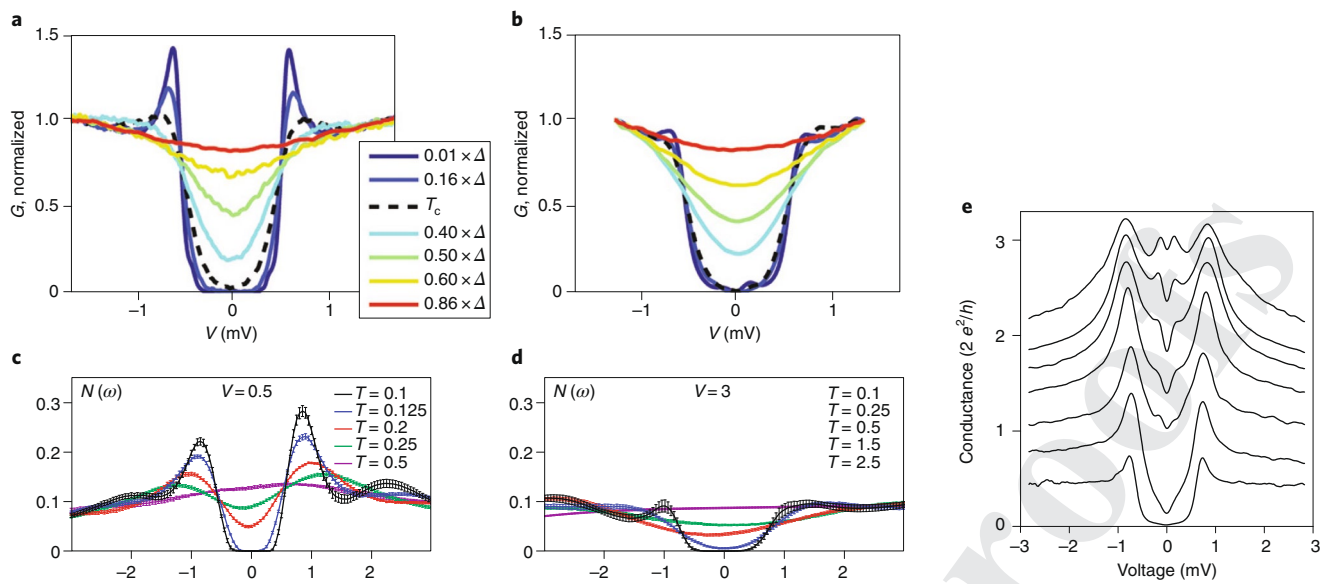


**Fig. 3 | Pseudogap and collective gap of preformed Cooper pairs.** **a, b**, Temperature evolution of the local tunnelling conductance  $G$  versus voltage bias  $V$ , characterized by the presence (**a**) or absence (**b**) of superconducting coherent peaks<sup>29</sup>. Both sets of data were measured at two different locations in superconducting samples. The tunnelling spectra are selected at temperatures equal to fractions of the low- $T$  spectral gap. The spectral gap values are  $\Delta = 560\mu\text{eV}$  and  $\Delta = 500\mu\text{eV}$  for **a** and **b**, respectively. The black dashed lines show the spectra measured at  $T_c$ . The clear pseudogap without coherence peaks and without a state at the Fermi level ( $V = 0$ ) is the signature of preformed Cooper pairs. Both sets of data are representative of superconducting samples with emergent granularity, for which superconducting islands show spectra with coherence peaks (**a**) and the surrounding matrix a gap without coherence peaks (**b**). The latter being a spectral signature of localized preformed Cooper pairs<sup>29</sup>. **c**, Numerical simulations of the disorder-averaged density of states  $N(\omega)$  for the 2D disordered attractive Hubbard model. A pseudogap develops for  $T \simeq T_c = 0.14$  and the coherence peaks vanish at  $T \sim T_c$ , in remarkable agreement with the experimental data in **a**. **d**, Similar simulations but for the insulating state at high disorder. The temperature evolution of  $N(\omega)$  resembles that of the superconducting case in **c** but without coherence peaks. This set of simulations indicate that the insulator is gapped due to electron pairing. **e**, Point contact Andreev spectroscopy: evolution of the local differential conductance  $G = dI/dV$  versus bias voltage measured on an a:InO sample at  $T = 0.065$  K and at the same position for different values of the point-contact conductance. The conductance curves are normalized to  $2e^2/h$  and have not been vertically shifted. The evolution from the tunnelling to the Andreev spectroscopy unveils a new pair of peaks inside the single-electron gap, which relate to the collective gap  $\Delta_{\text{col}}$ . Figure reproduced with permission from: **a, b**, ref. <sup>29</sup>, Springer Nature Ltd; **c, d**, ref. <sup>41</sup>, Springer Nature Ltd; **e**, ref. <sup>66</sup>, Springer Nature Ltd.

the resistance quantum  $h/(2e)^2$  for strongly disordered systems<sup>20</sup>. However, sometimes it is remarkably accurate, such as in the high- $T_c$  cuprate thin films<sup>21</sup> and some graphene tin-decorated hybrid devices<sup>22</sup>. But it can also approach  $h/e^2$  as observed in the disorder-tuned QBS in TiN thin films<sup>23</sup> without any metallic separator between the superconducting and insulating films, contrary to what is expected for the dirty boson model. Consequently, such a diversity of critical resistance values points towards the need to consider carefully ingredients other than just long-wavelength phase fluctuations. These additional ingredients may be system specific, which calls for less emphasis on the conjectured universal behavior, and more on the microscopics of the models for specific system classes.

**Amplitude-driven pathway.** The second major pathway to the QBS is based on the enhancement of the effective Coulomb repulsion due to the decrease in the diffusive motion of electrons<sup>13</sup>. This disorder-driven enhancement of the Coulomb interaction competes with the phonon-mediated attractive part of the interaction in the Cooper channel. The resulting continuous reduction of the effective attractive interaction leads to an amplitude-driven QBS, in practice a SMT with a vanishing pairing amplitude at the critical disorder. First calculated with a perturbative diagrammatic technique<sup>24,25</sup>, the full dependence of the critical temperature on the sheet resistance of the normal state,  $T_c(R_{\square})$ , was obtained via the renormalization group method by Finkel'stein<sup>4,5</sup>. This subsequently provided a simple analytical prediction for the critical disorder:

$g_c = 1/2\pi[\ln(1/T_{c0}\tau)]^2$ , where  $g = h/(e^2R_{\square})$  is the dimensionless sheet conductance. Remarkably,  $g_c$  is completely defined by only two parameters: the unsuppressed  $T_{c0}$  and the elastic scattering time  $\tau$ . The typical dependence of  $T_c$  on disorder is illustrated in Fig. 1b.

The Finkel'stein theory successfully describes the suppression of  $T_c$  in some thin films with low critical disorder<sup>5</sup>, defined as  $g_c \geq 4$ . In this case, the state found after terminating superconductivity is a 'bad' metal subject to weak localization effects at experimentally accessible temperatures. Its intrinsic mechanism, which is just an extension of mean-field Bardeen-Cooper-Schrieffer (BCS) theory including disorder-enhanced interaction, is expected to be somewhat universal. However, on a quantitative level, many systems exhibit a critical disorder beyond the range of applicability of the Finkel'stein theory ( $R_{\square} \sim h/4e^2$ ), where phase fluctuations are expected to contribute significantly<sup>3</sup>. When the sheet resistance reaches the resistance quantum, quantum phase fluctuations, localization effects and disorder-induced spatial inhomogeneities of the electronic properties disturb the standard dichotomy between phase and amplitude-driven pathways, leading to new scenarios where the two are intertwined.

**Emergent granularity of superconductivity at the local scale**

An early attempt to understand the diversity of experimental data on the QBS was to make a distinction between granular and homogeneous systems. The granular systems were usually thought of in analogy to Josephson tunnel-junction arrays, following a

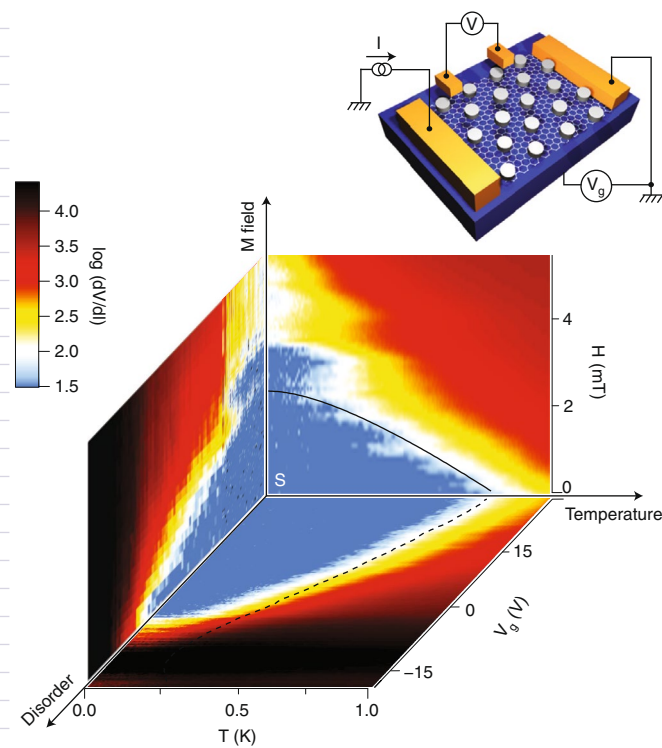


**Fig. 4 | Quantum breakdown of superconductivity in a mesoscopic device.**

A 3D phase diagram showing the superconducting state reconstructed from measurements of the array resistance in back-gate voltage,  $V_g$ , magnetic field,  $H$ , and temperature,  $T$ , space<sup>92</sup>. The resistance in  $(V_g, H)$  space is measured at 0.06 K. Notice that traces of a re-entrance of superconductivity above the first critical field are visible in both the  $(V_g, H)$  and  $(V_g, T)$  planes, a clear signature of the mesoscopic superconductivity<sup>57</sup>. Inset: a schematic of the mesoscopic sample — a graphene Hall bar decorated with an array of superconducting discs. Figure reproduced with permission from ref. <sup>92</sup>, Springer Nature Ltd.

phase-driven pathway to the breakdown of superconductivity. In contrast, the atomic structure of the homogeneous systems were expected to show ‘homogeneous’, short-range correlated disorder that should give rise to a homogeneous superconducting state, subject to Coulomb suppression of superconductivity. However, the last decade has unveiled a different, more complex and rich situation. In the strong scattering limit when the mean free path is of the order of the interatomic distance, disorder showed up as a strong disturbing agent that generates strong spatial fluctuations of the superconductivity-related spectral properties, enhanced by the proximity to the critical disorder<sup>26–34</sup>. Therefore, the classification between homogeneous and granular disordered materials became problematic because homogeneously disordered materials showed self-induced electronic inhomogeneities—that is, emergent granularity of the superconductivity—without an evident correlation with any structural granularity.

**Emergent superconducting granularity.** The concept of disorder-induced inhomogeneities of the superconducting state was proposed back in 1971 by Larkin and Ovchinnikov<sup>35</sup>. It was understood that relatively small spatial variations in the strength of the Cooper attraction  $\lambda(\mathbf{r})$  induced by disorder could lead to strong fluctuations of the local ‘transition temperature’  $T_c(\mathbf{r})$ . Since  $T_c(\mathbf{r}) \propto \exp(-1/\lambda(\mathbf{r}))$ , the variation in  $T_c$  is given by  $\delta T_c(\mathbf{r})/T_c \sim \delta\lambda(\mathbf{r})/\bar{\lambda}^2$  with the spatial average  $\bar{\lambda} \ll 1$ . These possible fluctuations and their impact on the superconducting properties have attracted considerable theoretical attention recently<sup>36–44</sup>.

The concept of spatial inhomogeneity of superconductivity was later analyzed within a different theoretical approach initiated by Ma and Lee<sup>45</sup>. Assuming that, for some reason, the Finkel’stein mechanism is ineffective, the destruction of superconductivity is considered to be the result of Anderson localization<sup>36,38,45–49</sup>. Earlier work<sup>36,38</sup> demonstrated, by numerically solving the self-consistent Bogoliubov-De Gennes equations, that in the presence of significant local disorder of the on-site electron energies, the order parameter defined as the quantum-statistical average,  $\Delta_{\text{op}}(\mathbf{r}) = \lambda\langle\psi_{\uparrow}(\mathbf{r})\psi_{\downarrow}(\mathbf{r})\rangle$ , becomes strongly inhomogeneous in space. Figure 2a shows the resulting fluctuations for the pairing amplitude calculated by Ghosal et al.<sup>36</sup>. Furthermore, the electron excitation spectrum of this inhomogeneous superconducting state has some unusual features: the spectral gap does not coincide with the order parameter, as it does for the standard BCS superconducting state, and the gap edge singularities (coherence peaks) in the density of states become smeared. The spatial fluctuations of the height of the coherence peak provides another indicator characteristic of the superconducting inhomogeneities.

The numerical simulations<sup>36,38</sup> demonstrated that sufficiently strong disorder suppresses the coherence peaks completely, while the spectral gap stays intact, thus opening an important question on the nature of the state terminating superconductivity. More recent numerical work<sup>40,41,43</sup>, including some based on the quantum Monte Carlo method<sup>41</sup> that takes into account the quantum phase fluctuations between the self-induced superconducting islands, showed that the ground state is an insulator with a spectral gap caused by the attractive interaction. This type of electron pairing is similar to the so-called negative- $U$  Hubbard model introduced by Anderson<sup>50</sup>.

The body of numerical work reviewed above demonstrates the concept of disorder-induced ‘emergent superconducting granularity’ and predicts new spectral features that contrast with the weak-disorder BCS superconductivity. However, numerical approaches are limited to small system sizes and to the strong coupling limit, whereas superconductivity is in essence a ‘weak effect’. Very recent results<sup>44</sup> indicate a way to solve this problem.

**Superconductivity near the mobility edge.** In order to make progress in understanding the strong-disorder regime, a combined analytical and numerical approach has been developed<sup>48,49</sup> to extend the theory of weak-coupling superconductivity. The crucial aspect of this new theoretical development lies in the fractal nature of the nearly localized electron wavefunctions when the Fermi level  $E_F$  is close to the Anderson mobility edge  $E_c$  (ref. <sup>51</sup>). These fractal electron wavefunctions  $\psi_i(\mathbf{r})$  feature many unusual properties including intensities  $\psi_i^2(\mathbf{r})$  that fluctuate very strongly in space (see Fig. 2b), multifractal statistics<sup>52</sup>, and matrix elements  $M_{ij} = \int d\mathbf{r}\psi_i^2(\mathbf{r})\psi_j^2(\mathbf{r})$  that grow as  $(E_c/\omega)^\gamma$  when the energy difference  $\omega$  between states  $i$  and  $j$  is small. In addition, right at  $E_F = E_c$  the inverse participation ratio  $P_i = \int d\mathbf{r}\psi_i^4(\mathbf{r})$  scales with the system size  $L$  as  $P \propto L^{-d_2}$ , where  $d_2$  is the fractal dimension related to the exponent  $\gamma = 1 - d_2/d$ . Note that the three-dimensional Anderson mobility edge is characterized by  $d_2 \approx 1.3$  and  $\gamma \approx 0.6$  (ref. <sup>52</sup>). Importantly, fractal properties of wavefunctions are very robust at strong disorder, even half-way the mobility edge<sup>51</sup>.

These unusual properties profoundly modify the superconductivity and have led to the concept of ‘fractal superconductivity’. Using a generalized mean-field theory, Feigel’man et al.<sup>49</sup> showed that the power-law scaling of  $M(\omega)$  leads to a new dependence of the critical temperature on the microscopic parameters:

$$T_c(\lambda) \sim E_F \lambda^{1/\gamma}. \quad (2)$$

This equation leads to the unexpected prediction that, for a constant  $\lambda$ , the critical temperature increases upon approaching the mobility edge compared to its weak disorder value. Later, the same enhance-

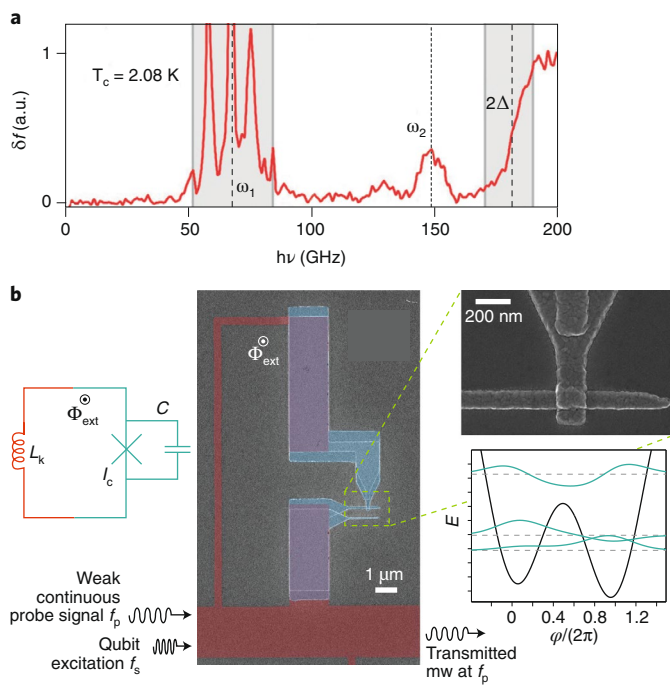


**Fig. 5 | Examples of applications of high microwave kinetic inductance**

**materials.** **a**, Typical absorption spectrum of a superconducting resonator made from granular aluminum in use for astronomical detectors and as superinductor, showing the conventional onset of absorption at  $2\Delta$  and subgap resonances<sup>112</sup>, identified as two distinct groups of absorption lines labeled as  $\omega_1$  and  $\omega_2$ . These modes are most likely collective modes coupled to the phase differences. The signal is the shift of the resonant frequency in the 2–6 GHz range due to the absorption of the radiation in the frequency range from 10–200 GHz. **b**, Hybrid RF SQUID used as a qubit and consisting of an Al SIS superconducting tunnel junction, shunted by a high kinetic inductance loop made of TiN. Figure reproduced with permission from: **a**, ref. <sup>112</sup>, APS; **b**, ref. <sup>106</sup>, Springer Nature Ltd, under CC-BY-4.0.

ment of  $T_c$  due to fractality was addressed by means of the renormalization group approach<sup>53,54</sup> in the 2D limit. It was shown that the partial suppression of the (screened) Coulomb amplitude makes the enhancement of  $T_c$  by disorder possible in two dimensions as well.

The results of refs. <sup>48,49,53,54</sup> were obtained within a generalized mean-field approximation that neglects thermal phase fluctuations<sup>12</sup>. However, it was shown in ref. <sup>49</sup> that the intensity of the phase fluctuations is only moderate for superconductivity at the mobility edge, so the major conclusion about the  $T_c$  enhancement is valid. On the other hand, phase fluctuations do become crucial and destroy superconductivity when the Fermi level moves sufficiently far into the Anderson-localized band.

Another important feature of superconductivity near the mobility edge is the highly inhomogeneous superconducting order parameter. The dispersion  $\sqrt{\langle \Delta^2(\mathbf{r}) \rangle}$  of the order parameter  $\Delta(\mathbf{r})$  is much larger<sup>49</sup> than its mean value  $\langle \Delta(\mathbf{r}) \rangle$ , leading to a picture of a superconducting state splintered into superconducting islands. Such a strongly inhomogeneous superconductivity is a direct consequence of the fact that fractal wavefunctions occupy only a small fraction of the available volume (Fig. 2b). A direct consequence of the inhomogeneity of  $\Delta(\mathbf{r})$  is a strong vortex pinning and measurable critical currents even extremely close to the upper critical field<sup>55</sup>.

**Emergent granularity within the amplitude pathway.** The theoretical approaches reviewed above predicted the emergence of an inhomogeneous superconducting state in the strong disorder limit.

However, these theories do not include the unavoidable Coulomb interaction that affects the attractive coupling via Finkel'stein's mechanism. Solving the combined effect of Anderson localization and Coulomb interaction is known to be a notoriously difficult task that has not yet been accomplished. Nevertheless, some progress<sup>39</sup> was made on the perturbative level by including quantum interference effects—the universal conductance fluctuations—to Finkel'stein's theory of the SMT. This extended Finkel'stein theory predicts significant spatial fluctuations of the local transition temperature on approaching the quantum critical point of the theory,  $g_c$ , due to the disorder enhancement of the mesoscopic fluctuations of the effective Coulomb amplitude. The fluctuations of  $T_c$  are given by  $\frac{\delta T_c}{T_c} \approx \frac{0.4}{g(g-g_c)}$ , which shows that these fluctuations necessarily become strong upon approaching the quantum critical point. This is illustrated by the shaded region around the mean  $T_c$  in Fig. 1b.

**Intermediate conclusion regarding the theory.** The major outcome of these recent theoretical developments is a clear breakdown of the conventional dichotomy between the amplitude- and phase-driven pathways. An initial normal state with homogeneous electronic properties can yield an inhomogeneous superconducting state whose spatial fluctuations get enhanced in the vicinity of the critical disorder. This formation of superconducting islands immersed in a non-superconducting matrix that would be metallic in the Finkel'stein SMT scenario and insulating in the strong disorder limit, intimately involves phase fluctuations between the weakly-coupled superconducting islands. A new scenario has emerged that involves a remarkably complex and subtle interplay between localization phenomena (effect of disorder and multifractality), Coulomb interaction and phase fluctuations. The breadth of consequences of these superconducting inhomogeneities on the transport and thermodynamic properties is not yet understood and will certainly produce new conceptual advances. In addition, it makes the system sensitive to external conditions in a variety of experiments.

We briefly mention a few more theoretical consequences. The spontaneous formation of superconducting islands leads to an enhancement<sup>56</sup> of the electron dephasing rate  $1/\tau_\phi$  at low temperatures. Andreev reflections of electrons between the superconducting islands (with uncorrelated fluctuations of their phases) become the dominant mechanism of decoherence<sup>56</sup>, far exceeding the usual Coulomb contribution  $1/\tau_\phi^C \sim T/g$ . This has implications for the possible existence of some anomalous metallic phases<sup>9</sup>. Under a perpendicular magnetic field, the self-induced inhomogeneities are predicted to induce multiple reentrant superconducting phases above the upper critical field in mesoscopic samples<sup>57</sup>. More generally, disorder-induced inhomogeneities lead<sup>58</sup> to the breakdown of the scaling theory<sup>39</sup> of the quantum SMT, which states that large-scale superconducting fluctuations are irrelevant due to long-range of proximity coupling via the metal matrix.

### Real-space visualization of superconducting inhomogeneities.

In experiments, a continuous reduction of  $T_c$  with increasing sheet resistance, consistent with Finkel'stein's theory, has long been the hallmark of structurally homogeneous materials<sup>15,60</sup>, and, consequently, assumed homogeneous superconductivity. Progress in low-temperature scanning tunnelling microscopy means that the local density of states can be measured with sub-kelvin resolution. These tunnelling experiments have shed new light on this assumed homogeneity and have revealed an emergent granularity of superconductivity on the local scale.

In 2008, Sacépé et al.<sup>26</sup> reported the first scanning tunnelling spectroscopy of thin superconducting films near the QBS. They studied TiN films, which exhibit a QBS<sup>23</sup> with a continuous reduction of  $T_c$  and a high critical disorder of the order of 30kΩ. The spectra of the local tunnelling density of states revealed significant spatial fluctuations of the superconducting gap  $\Delta(\mathbf{r})$  on the scale of

tens of nanometers. Figure 2c shows a typical spatial map of  $\Delta(\mathbf{r})$  measured at 0.05K. Upon approaching the critical disorder, these fluctuations were shown to increase from  $\delta\Delta(\mathbf{r})/\Delta \simeq 0.15$  ( $\Delta$  is here the average superconducting gap) for an intermediate disorder ( $T_c \simeq 0.3T_{c0}$ ) up to  $\delta\Delta(\mathbf{r})/\Delta \simeq 0.5$  for a nearly critical sample with  $T_c \simeq 0.1T_{c0}$ . Similar results were obtained in a series of studies by Raychaudhuri and co-workers on thick NbN films<sup>30,43</sup> and by Roditchev and co-workers<sup>32,61,62</sup> on ultra-thin NbN films where the initial suppression of  $T_c$  with disorder also seems to follow the amplitude pathway. Cabrillet et al.<sup>61</sup> combined topography and scanning tunnelling spectroscopy data to demonstrate the absence of any spatial correlation between small-scale structural grains and larger-scale fluctuations of the gap  $\Delta(\mathbf{r})$ . In a more recent work, Cabrillet et al.<sup>62</sup> also showed a clear anti-correlation between the width of the gap and the slope of the high-voltage anomaly in the tunnelling conductance, attributed to the ‘soft Coulomb gap’<sup>63</sup>. This anti-correlation can be accounted for because regions with larger local resistance are expected to have smaller  $\Delta(\mathbf{r})$  due to the disorder-enhanced Coulomb effects<sup>45</sup>. Measurements in a magnetic field add an additional perspective to this picture. Ganguly et al.<sup>33</sup> showed that NbN films far from the QBS that exhibit uniform superconducting properties at  $B = 0$  develop strong spatial inhomogeneities under perpendicular magnetic field values of 4 to 7.5 T, in agreement with theory<sup>57,64</sup>.

In general, the experiments on both TiN (ref. 26) and NbN (refs. 32,33,43,61,62) films demonstrate the same trend. An increase of the sheet resistance close to  $R_Q = h/4e^2$  and a related suppression of  $T_c$  are systematically accompanied by an increase of the gap fluctuations  $\Delta(\mathbf{r})$ . Furthermore, the coherence peaks also fluctuate spatially and provide a measure of the amplitude of the local order parameter<sup>29,43</sup>.

The disorder-induced enhancement of the superconducting gap inhomogeneities is accompanied by a significant increase of the ratio  $\Delta/T_c$  in TiN films (ref. 26), NbN (ref. 28) and in MoGe (ref. 65), upon approaching the critical disorder. In TiN films, it grows up to a value of 4, far above the weak-coupling value of 1.76. This indicates a serious deviation from the standard ratio of the BCS theory. The same evolution is seen in a:InO films that are much thicker than the superconducting coherence length<sup>29,66</sup>. In this case the ratio of the spectral gap to  $T_c$  grows from 2.5 to 5.5 when  $T_c$  is reduced from 3.5 K to 1.2 K by increasing disorder.

A remarkable consequence of the increase of  $\Delta/T_c$  with disorder is the non-vanishing spectral gap in nearly critical samples in spite of the enhanced spatial fluctuations. The anomalously large and increasing  $\Delta/T_c$  ratio indicates that, at the critical disorder defined by  $T_c = 0$ , the spectral gap remains finite and potentially persists into the insulator phase<sup>26,31</sup>. This behaviour would be consistent with the prediction of a gapped insulating phase (Fig. 3d) in the disordered attractive Hubbard model<sup>36,38,41</sup> discussed in the previous section. Furthermore, as shown in a:InO<sup>29</sup>, locations with a vanishing local order parameter—evidenced by a lack of coherence peaks—remain fully gapped, although other materials have sub-gap states<sup>26,30,32,43,62,67</sup>. The origin of the sub-gap states in nearly critical films with very low  $T_c$  remains unclear but could be the result of pair breaking due to interactions<sup>68</sup>, or more trivially limited by the energetic resolution of tunnelling spectroscopy, which is known to be notoriously sensitive to the filtering of the electromagnetic environment<sup>69,70</sup>.

Recently, Zhao et al. used low-temperature scanning tunnelling spectroscopy to investigate an epitaxial monolayer of NbSe<sub>2</sub>, on which disorder was controlled through in situ adatom deposition prior to tunnelling measurements<sup>34</sup>. They observed an initial increase of the superconducting gap with disorder, followed by a sharp drop, as shown in Fig. 2d. This may possibly constitute evidence for enhancement of 2D superconductivity by disorder<sup>53</sup>, although additional checks for alternative mechanisms are needed.

These scanning tunnelling experiments provided compelling evidence for the emergent superconducting granularity in

homogeneously disordered materials. The new picture of the superconducting state in the vicinity of the QBS is that of superconducting puddles embedded in a matrix with vanishing local order parameter, a matrix that can be gapped or gapless in case of a SIT or SMT, respectively. Consequently, quantum phase fluctuations in such weakly coupled puddles will definitely be crucial in the ultimate suppression of superconductivity. These superconducting inhomogeneities that emerge near criticality lead us to conclude that there is a progressive evolution from amplitude-driven to phase-driven mechanisms of QBS upon increasing disorder, at least in TiN, NbN and a:InO, the materials investigated so far.

### Preformed pairs and their localization at the QBS

In strongly disordered superconductors one can not a priori assume that the attractive interaction leading to Cooper pair formation is uniformly spread through the material. One possibility is that the attractive interaction fluctuates from one point to another with a significant amplitude so that the Cooper pairs are formed locally. As this situation does not necessarily lead to long range coherence, these pairs are called ‘preformed pairs’, anticipating the development of a state of superconductivity by phase coherence between these localised pairs. Such a theoretical possibility, which is obviously difficult to identify based on transport measurements, has recently received experimental support from local spectroscopy data. A suppression of the quasiparticle tunnelling density of states was observed at temperatures far above the superconducting transition temperature, in strongly disordered TiN thin films<sup>27</sup>. A similar suppression is routinely observed in underdoped cuprate superconductors and labeled a ‘pseudo-gap’<sup>71</sup>. Assuming that this pseudo-gap (PG) is related to superconductivity, one is led to conclude that on cooling down, first the preformed pairs of electrons appear, and then they become coherent at much lower temperatures, at the critical temperature  $T_c$ . An early theoretical analysis of the tunnel current above  $T_c$  in the regime of superconducting fluctuations was carried out by Varlamov and Dorin<sup>72</sup>, and showed an apparent pseudo-gap formation.

The presence of preformed electron pairs in a conventional low- $T_c$  superconductor with strong disorder was suggested by experiments of Sacépé et al.<sup>29</sup> in scanning tunnelling measurements on a:InO films. A nearly full-width tunnelling gap,  $\Delta_{PG}$ , was visible at the temperature where zero resistance develops, defined as  $T_c$ , while a considerable suppression of the density of states was detected up to temperatures of  $4T_c$ . Right below  $T_c$  coherence peaks developed near the edges of the gap at a number of locations of the investigated area, while at other points no coherence peaks are found down to the lowest  $T \ll T_c$ . These observations, summarized in Fig. 3a,b, stimulated the theory of the QBS, to be discussed below. Similar pseudo-gap-type features were reported in subsequent experiments on a:InO, by Sherman et al.<sup>31</sup>, on NbN, by Mondal et al.<sup>28</sup>, Chand et al.<sup>30</sup>, and Cabrillet et al.<sup>61,62</sup>, and on MoGe by Mandal et al.<sup>73</sup>. In all cases, the observations are carried out on films with a  $T_c$  strongly suppressed by disorder.

In interpreting these experiments, it is reasonable to assume that a relatively large tunnelling gap is related to electron pairing, but it cannot serve as a direct measure of the superconducting coherence. In addition, the value is too large in comparison to superconducting transition temperature  $T_c$  to be understood by the BCS-type theory or its extensions like the Eliashberg theory. Eventually, numerical work showed<sup>38,41</sup> that the single-particle gap survives into the range of strong disorder, without the typical indications of superconducting coherence. An alternative interpretation of the data has been suggested, where the suppression of the tunnelling density-of-states near the Fermi-energy is due to the dynamical Coulomb blockade<sup>63,74</sup>. However, in low- $T_c$  disordered superconductors, it is experimentally not difficult to distinguish between dynamical Coulomb blockade and superconductivity-related pseudo-gap, due to the large difference in relevant energy scales: about 1 meV for

434 pseudo-gap and on the order of 0.1 meV for dynamical Coulomb  
435 blockade. An example of a joint analysis of dynamical Coulomb  
436 blockade together with the Finkelstein mechanism of superconductivity  
437 suppression has recently been discussed by Carbillet et al.<sup>62</sup>.  
438 We believe that a theory based on preformed Cooper pairs is the  
439 most plausible candidate.

440 We proceed by addressing the formation of a collective gap  
441 for the condensation of the preformed Cooper pairs. Within BCS  
442 theory, the collective gap  $\Delta_{\text{col}} = 2\Delta_{\text{BCS}}$ , corresponds to the minimal  
443 excitation energy above the superconductive ground state,  
444 if single-particle excitations are forbidden. Experimentally, as  
445 proposed by Deutscher<sup>75,76</sup>, the collective gap of cuprate superconductors  
446 can be measured by point contact spectroscopy  
447 using Andreev reflection. The voltage threshold for two-electron  
448 transfer,  $2eV_{\text{col}} = 2\Delta_{\text{col}}$ , which coincides with the threshold for  
449 single-electron tunnelling  $eV = \Delta_{\text{BCS}}$ , if the BCS relation is valid.

450 A similar idea was implemented recently by Dubouchet et al.<sup>66</sup>  
451 for a:InO close to the QBS. The point-contact differential conduc-  
452 tance  $dI/dV$  was measured starting from the purely tunnelling  
453 regime to a highly transmissive regime with a contact resistance  
454 of a few k $\Omega$ , at which both single-electron and Andreev processes  
455 are relevant. In the highly-transmissive regime, additional peaks  
456 emerged in  $dI/dV$  (Fig. 3e) at low voltages,  $eV_{\text{col}} \ll \Delta_{\text{PG}}$ , and only  
457 in the superconducting state. Moreover,  $V_{\text{col}}$  was found to be weakly  
458 dependent on the tip location, but strongly temperature-dependent,  
459 similar to the  $\Delta_{\text{BCS}}(T)$  dependence. Both features are in contrast  
460 with the behavior of the single-particle threshold  $\Delta_{\text{PG}}$ . The mag-  
461 nitude of  $\Delta_{\text{col}} \equiv eV_{\text{col}}$  was interpreted as a genuine collective gap  
462 that develops together with the macroscopic superconducting  
463 coherence. This type of behaviour was found only for strongly  
464 disordered a:InO films. In contrast, less disordered films (with  
465  $T_c \geq 3\text{K}$ ) demonstrate single-gap BCS-type behaviour without any  
466 pseudo-gap feature.

467 These observations were analyzed by invoking the notion of the  
468 ‘parity gap’,  $\Delta_{\text{par}}$ , introduced in the seminal paper of Matveev and  
469 Larkin<sup>77</sup>, who developed the theory for an ultra-small supercon-  
470 ducting grain. For sufficiently small grains the single-electron level  
471 spacing  $\delta_1 = 1/\nu\mathcal{V}$  ( $\nu$  the density-of-states per unit of volume and  
472  $\mathcal{V}$  the volume of the grain) exceeds the value of the superconduct-  
473 ing gap  $\Delta_0$  of the bulk of the material. The level spacing  $\delta_1$  does not  
474 exceed the Debye energy. The condition  $\delta_1 \gg \Delta_0$  prevents the for-  
475 mation of many-body coherence, of the numerous single-electron  
476 states. However two electrons, residing in the same localized orbital  
477 state with opposite spins, still attract each other and gain some  
478 energy  $\Delta_{\text{par}} \propto \delta_1$ , with respect to the case when those electrons  
479 populate different localized orbitals.

480 We implement the idea of the parity gap to describe the  
481 pseudo-gap in strongly disordered bulk (or 2D) materials follow-  
482 ing Ma and Lee<sup>45</sup>, Ghosal et al.<sup>38</sup>, and Feigelman et al.<sup>48,49</sup>. We  
483 assume, going beyond the theory described in Section IV, that the  
484 Fermi level for non-interacting electrons lies in the localized part  
485 of the band, but close to the mobility edge  $E_c$ . The single-electron  
486 eigenfunctions are localized, with relatively long localization length  
487  $L_c \sim l[(E_F - E_c)/E_c]^{-\nu}$ , where the exponent  $\nu \approx 1.5$  in 3D. Then  
488 the matrix elements  $P_i = \int d\mathbf{r} \psi_i^\dagger(\mathbf{r})$  are non-zero in the thermo-  
489 dynamic limit and scale as  $P_i \propto L_c^{-d/2} \sim [(E_F - E_c)/E_c]^{-\nu d/2}$ , due to  
490 the fractal nature of the electron eigenfunctions. The parity gap due  
491 to the local attraction between two electrons  $\Delta_{\text{par}} = \lambda/\nu P_i$  scales  
492 in the same way. This situation, similar to the one for ultra-small  
493 grains<sup>77</sup>, is realized when the single-electron spacing  $\delta_1 = (\nu L_c^d)^{-1}$   
494 far exceeds the transition temperature  $T_{c0}$  for the critical disorder  
495 ( $L_c \rightarrow \infty$ ), see equation (2). Then it is possible to show<sup>49</sup> that the  
496 value of the parity gap  $\Delta_{\text{par}}$  lies between two other energy scales:

$$T_{c0} \ll \Delta_{\text{par}} \sim \delta_1 \left( \frac{T_{c0}}{\delta_1} \right)^\gamma \ll \delta_1 \quad (3)$$

When such a bulk disordered system, with a tendency to electron  
pairing, does not develop superconducting coherence, the parity  
gap is seen both as a pseudo-gap in tunnelling experiments, and as  
an activation gap in transport.

This physically rich theoretical model was developed to reach an  
understanding of the experimental data on a:InO (refs.<sup>78,79</sup>). Large  
activation gaps, up to 10–15 K, were reported in electronic trans-  
port measurements. It was noted by Shahar and Ovadyahu<sup>78</sup> that the  
experimental data rules out conventional scaling of the activation gap  
 $\propto \delta_1$ . Feigelman et al.<sup>49</sup> argued that the same data are consistent with a  
modified scaling of  $\Delta_{\text{par}}$  presented in equation (3). Superconductivity  
will coexist with a parity gap when the ratio of  $\delta_1/T_{c0}$  is not too large.  
The very presence of a solution with nonzero  $T_c$  much smaller than  
both  $\Delta_{\text{par}}$  and  $\delta_1$  is a new feature of the theory of ref.<sup>49</sup> that was not  
anticipated in the original approach by Ma and Lee<sup>45</sup>. It is due to two  
effects that enhance the overlap matrix elements  $M_{ij}$ : the fractal nature  
of the eigenfunctions, and the Mott resonances<sup>80</sup> between localized  
eigenstates with a small energy difference  $\omega \ll \delta_1$ . The collective gap  
 $\Delta_{\text{col}}(T)$  at  $T \ll T_c$  appears to be of the same order as  $T_c$ , and much  
less than  $\Delta_{\text{par}}$ . An additional feature expected for the pseudo-gapped  
superconductors is the violation of the usual BCS rule that the full  
optical spectral weight is insensitive to superconducting transition<sup>49</sup>.  
Upon a further increase of disorder and of the level spacing  $\delta_1$ , the  
transition temperature  $T_c$  and the collective gap  $\Delta_{\text{col}}$  gets smaller and  
eventually vanishes, while  $\Delta_{\text{PG}}$  stays nonzero<sup>41,49</sup>. The resulting ground  
state is an insulator with preformed electron pairs.

For a system with preformed electron pairs, close to the QBS,  
the values for both  $T_c$  and  $\Delta_{\text{col}}$  are much smaller than the pseu-  
dopgap  $\Delta_{\text{PG}}$ . Therefore, this transition can be understood in terms  
of the Anderson pseudo-spin model<sup>81</sup>, which describes hop-  
ping of the preformed pairs between different localized orbitals  
 $\psi_i(\mathbf{r})$ . This specific case of the QBS can be called a ‘pseudo-spin’  
QBS. The hopping terms in the effective Hamiltonian are given by  
 $H_{\text{hop}} = -\sum_{ij} J_{ij} (S_i^+ S_j^- + \text{h.c.})$  where  $S_i^\pm$  are the creation and anni-  
hilation operators of a preformed pair in the  $i$ th orbital. These hop-  
ping terms compete with the random on-site potential energy given  
by  $H_{\text{loc}} = \sum_i 2\xi_i S_i^z$ . The preformed pairs are just hard-core bosons,  
and hence the operator set  $S_i^z, S_i^+, S_i^-$  is formally equivalent to the  
spin- $\frac{1}{2}$  operators  $S_i$ . The superconducting state is then described  
by the non-vanishing quantum-statistical average values such as  
 $\Delta_i = \langle S_i^- \rangle$ , while in the insulating state all  $\Delta_i \equiv 0$  and the preformed  
pairs are localized.

This pseudo-spin QBS appears to be in the same universality  
class as the order-disorder transition in the quantum XY spin- $\frac{1}{2}$   
model with random transverse fields. The transition is controlled  
by the value of the effective coupling strength  $J \sim ZJ_{ij}$ , with  $Z$  the  
typical number of connections per ‘spin’. The theory worked out by  
Mézard, Ioffe and Feigelman<sup>82</sup> leads to the following conclusions:

- A  $T = 0$  transition between superconducting and insulating  
states occurs at some critical value of the coupling strength  $J_c$ .
- At  $J > J_c$ , the superconducting state exists below a critical  
temperature  $T_c(J)$ , whose magnitude drops very sharply to zero  
when  $J \rightarrow J_c$ .
- In a wide range of  $J > J_c$ , the ordered state is extremely inho-  
mogeneous, with a very broad probability distribution  $\mathcal{P}(\Delta_i)$ .  
Subsequent numerical studies for a 2D model by Lemarié et al.<sup>43</sup>  
have confirmed this result.
- A typical value of the order parameter  $\Delta_{\text{typ}} = \exp(\overline{\ln(\Delta_i)})$  dem-  
onstrates an unusual exponential scaling near the  $T = 0$  criti-  
cal point:  $-\ln \Delta_{\text{typ}} \propto (J - J_c)^{-1}$ . This type of scaling was found  
earlier by Carpentier and Le Doussal<sup>83</sup> for the disorder-driven  
Berezinskii–Kosterlitz–Thouless transition.

We would like to draw the attention to several unusual and  
important predictions of this pseudo-spin QBS. Firstly, the inhom-

generality of all superconducting properties close to the pseudo-spin QBS is much stronger than the emergent granularity in the bulk of the superconducting region. Moreover, the former develops at much larger spatial scale, which diverges close to the QBS. Eventually, the pseudo-spin QBS acquires superconducting features which are reminiscent of the classical percolation transition. This aspect might provide a framework to understand the unexpected size effects found near the QBS by Kowal and Ovadyahu<sup>84</sup>, as well the unusual behavior of the Nernst coefficient at  $T \gg T_c$  in near-critical a:InO films<sup>85,86</sup>.

The mechanism we have described for the pseudo-spin QBS has one common feature with the ‘bosonic’ scenario. In essence, hard-core bosons defined on a lattice are formally equivalent to spin-1/2 spins sitting on lattice sites. The crucial physical difference is that the pseudo-spin scenario does not assume any local superconducting order with many-body correlations unless global superconductivity has developed. In particular, no trace of the coherence peaks is expected in the insulating state, in contrast to the standard bosonic scenario based on the Josephson tunnel-junction model: The superconducting grain of a size large enough to have  $\delta_1 \ll \Delta$  would show smeared coherence peaks in the tunnelling conductance on either side of the QBS.

Another important feature of the pseudo-spin scenario for the QBS is that disorder plays a crucial role, unlike the commonly used Coulomb-blockade, Josephson tunnel-junction model. The pseudo-spin QBS model we describe here is in that sense similar to the infinite-disorder renormalization group theory<sup>87,88</sup>. The strong disorder effects and the need to account for the whole probability distribution of the relevant variable<sup>83,89</sup> make the use of an elementary scaling analysis problematic near such phase transitions. This might be the reason for the broad range of critical exponents found in the literature.

### Mesoscopic approach to inhomogeneous superconducting materials

A major research direction in the past few decades has been on networks of superconducting islands coupled by tunnel barriers through which Josephson tunnelling can occur<sup>8</sup>. The main emphasis was on an analysis based on Berezinskii–Kosterlitz–Thouless physics, the competition between Coulomb blockade and Josephson coupling, and the magnetic field dependence expressed as the number of flux quanta per closed loop of the network. They have been also used as model systems to understand the QBS in real materials. While these systems are useful, these tunnel-junction-based systems ignore two important ingredients that are relevant for real materials. One ingredient is the use of large superconducting islands with a well-defined macroscopic quantum phase. In practice, much smaller pockets of superconductivity with a small number of electrons with a poorly defined phase may occur. Secondly, the coupling between the islands might in practice be much more transmissive than for a tunnel barrier, either because of a few transmissive quantum channels or by a diffusive proximity effect. These arrays were first made several decades ago<sup>90</sup> and were recently addressed, with better lithography, in the work by Eley et al.<sup>91</sup>. In the latter work a series of samples was studied with different coupling strengths between the islands, due to a variation in distance between the superconducting islands. The analysis was, as in the earlier work, based on the thermal Berezinskii–Kosterlitz–Thouless phase transition, assuming a Ginzburg–Landau proximity-effect description, with the coupling strength varying exponentially with distance.

The discovery of tunable 2D materials such as graphene in combination with superconductors makes it possible to construct a Josephson arrays where the coupling strength can be tuned in situ. This has been realized in a recent experiment by Han et al.<sup>92</sup>. A layer of graphene was decorated with a triangular array of circular tin disks, each with a diameter of 400 nm and a mutual distance

between the centers of the disks of 1  $\mu\text{m}$ . The total number of disks covered an area of  $5 \times 10 \mu\text{m}^2$ . The sample was equipped with a gate that allowed the tuning of the carrier density in the graphene, which meant that the Josephson coupling could be tuned. The conductivity of the array could be tuned from a full superconducting state through an ‘anomalous metal’ phase, going over to an approximate insulating phase, with diffusive transport in the graphene. The data as a function of gate voltage for different magnetic fields and temperatures clearly resemble (Fig. 4) the phase diagram laid out by M. Fisher<sup>6</sup>. These results are already interesting and important as such, showing the importance of quantum phase fluctuations in Berezinskii–Kosterlitz–Thouless physics, but the experimental method allows for several other routes to be explored. In principle, one could consider smaller islands in order to get the islands with an energy spacing for the electrons larger than the superconducting energy gap, although this might require the use of superconductors with a low carrier density. A second route is to use ballistic graphene, which is in principle possible by encapsulating the graphene in exfoliated boron nitride. Thirdly, the small scale of the array, about 20 sites, may lead to a contribution from finite-size effects on the observed quantum Berezinskii–Kosterlitz–Thouless-like transition. These need to be evaluated by making arrays with more sites.

Böttcher et al.<sup>93</sup> carried out a similar experiment using a rectangular array of square-shaped superconducting aluminium islands deposited on a tunable two-dimensional electron gas in the semiconductor InGaAs system, using the materials systems developed for Majorana physics. The published results are analogous to data presented in earlier work on other 2D arrays and analyzed by the conventional scaling analysis<sup>6</sup>. In principle this experimental system has the potential to benefit from insights in mesoscopic superconductivity. The Andreev reflection process which mediates the phase coupling between the superconducting islands has been thoroughly analyzed by Kjaergaard et al.<sup>94</sup>. The critical new step is to integrate the understanding of the proximity effect from the perspective of Andreev processes at the interface between the normal metal and the superconductor. This knowledge is well-developed and continues to be tested in various hybrid systems. The important ingredient of the study of Josephson-coupled arrays is the fate of the quantum phase of each superconducting island. Further research, with considerably smaller superconducting islands appears to be within reach.

The emphasis on the tunability of the Josephson coupling energy in controlling the macroscopic transport properties of the arrays highlights the need for a full understanding of the dependence on environmental noise. Martinis and co-workers<sup>70,95</sup> have addressed this subject in the context of macroscopic quantum tunnelling. Additionally, the thermal blackbody radiation was found to contribute significantly to the performance of superconducting quantum circuits<sup>96</sup>. A reminder of the importance of the sensitivity to environmental radiation for materials research was shown in recent experiments by Tamir et al.<sup>10</sup>, which showed it in the resistive transition of a:InO, but also of a crystalline 2D superconductor, H<sub>2</sub>-NbSe<sub>2</sub>. A similar dependence was found recently by Dutta et al.<sup>11</sup> in the onset of resistance in the vortex state of a-MoGe films. It is a reminder that experiments on ‘weak’ superconductors, on the verge of quantum breakdown, need to be carried out in an electromagnetically well-shielded cryogenic environment, common for mesoscopic research but not typical for materials research.

### Applications to quantum circuits and qubits

One of the most interesting and fascinating potential applications of strongly disordered superconductors is the superinductor. A superinductor is a non-dissipative element of an electrical circuit with an impedance that depends on the capacitance  $C$  and inductance  $L$  as  $Z = \sqrt{(L/C)}$ , and is much larger than the resistance quantum  $R_Q = h/(2e)^2$ . The inductance of a superconducting wire consists of the geometric inductance, which stores the energy of the

566 electromagnetic field, and the kinetic inductance of the supercon-  
 567 ducting condensate, which stores the kinetic energy of the mov-  
 568 ing superfluid. The geometric inductance scales with the length of  
 569 the wire and depends only logarithmically on the diameter of the  
 570 wire. Its value is typically  $1 \text{ pH } \mu\text{m}^{-1}$ , which makes the geometric  
 571 inductance unusable, a problem well known in for example RF  
 572 electronics<sup>97</sup>. The alternative is to exploit the kinetic inductance of  
 573 a low-dimensional material such as graphene<sup>97</sup>, which for normal  
 574 conduction leads to high losses and hence low quality factor if used  
 575 <sup>91d</sup> in a resonator. The low loss can be provided by a superconductor of  
 576 which the kinetic inductance is in general given by  $L_k = \hbar R_n / \pi \Delta$ ,  
 577 which means that a high normal state resistivity and a low super-  
 578 fluid density can be used to maximize the kinetic inductance.  
 579 Ideally, one would like to achieve at least an inductance per unit  
 580 length of  $0.1 \text{ nH } \mu\text{m}^{-1}$ , which implies that films with  $0.5 - 2.5 \text{ nH } \square$   
 581 are required. With such a superinductor one can construct pro-  
 582 tected qubits reviewed by Doucot and Ioffe<sup>98</sup>, with new ideas put  
 583 forward by Brooks et al.<sup>99</sup>, Groszkowski et al.<sup>100</sup> and Smith et al.<sup>101</sup>.

584 Motivated by these ideas about protected qubits and another  
 585 proposal put forth by Mooij, Nazarov and Harmans<sup>102,103</sup> on quan-  
 586 tum phase slip junctions, Astafiev and co-workers have studied the  
 587 quantum coherence of superconducting nanowires for a range of  
 588 materials like a:InO (ref. <sup>104</sup>), NbN (ref. <sup>105</sup>), and TiN (refs. <sup>106,107</sup>).  
 589 They considered coherent quantum phase slip processes, rather  
 590 than thermally activated phase slips. The critical quantity is the  
 591 transition amplitude for quantum phase slips, expressed in energy  
 592 as  $E_s$ , reaching values in the 100 GHz range. In addition, one needs  
 593 an impedance of the environment larger than the quantum unit of  
 594 resistance of  $6.45 \text{ k}\Omega$ . The scale of the inductive energy  $E_L$  is given  
 595 by  $\Phi_0^2 / 2L$  with  $L$  the kinetic inductance of the wire. In order to  
 596 reach  $E_s \gg E_L$  one needs superconducting materials with a high  
 597 normal state resistivity, such as strongly disordered superconduc-  
 598 tors, which are central in this review (Fig. 5b).

599 An alternative experimental strategy is the work of Kuzmin  
 600 et al.<sup>108</sup>. Instead of a model system to study the breakdown of super-  
 601 conductivity they constructed a model system in which they could  
 602 experimentally focus on the collective electromagnetic phase mode.  
 603 They created a linear chain of 40,000 Josephson tunnel junctions  
 604 and used the device to study the collective modes of microwave pho-  
 605 tons. These modes have a velocity as low as  $v \approx 10^6 \text{ m s}^{-1}$  and a wave  
 606 impedance as high as  $Z \approx R_Q$ , with  $R_Q = h / (2e)^2 \approx 6.5 \text{ k}\Omega$ , the  
 607 superconducting resistance quantum. A SIT is obtained by chang-  
 608 ing the area of the junction<sup>108</sup>, which leads to a smaller area in which  
 609 the charge can be quantised on the superconducting island, and  
 610 hence to strong fluctuations of the quantum phase on the islands,  
 611 visible, for example, as a breakdown of the collective modes.

612 In the search for suitable materials, thin films of granular alu-  
 613 minium (GrAl) are being explored as a possible candidate<sup>109-111</sup>.  
 614 This subclass of materials has been known for a long time to be  
 615 easily accessible, but at the same time difficult to understand. The  
 616 material is made by depositing aluminium in a partial pressure  
 617 of oxygen leading to an assembly of small aluminium grains, sur-  
 618 rounded by an  $\text{AlO}_x$  layer, hence the name 'granular'. For increasing  
 619 resistivity the critical temperature increases up to a large factor of 3  
 620 to 4, an observation that has so far defied a convincing explanation.  
 621 A number of promising properties have been measured, at the same  
 622 time some detrimental properties have also been identified, includ-  
 623 ing the microwave properties<sup>112</sup> (Fig. 5a). The same material is also  
 624 studied by Gershenson and co-workers<sup>113,114</sup>. The parameter details  
 625 for granular aluminium are not very well known. It is possible that  
 626 they can be considered as random arrays of tunnel junctions, small  
 627 aluminium particles surrounded by an oxide tunnel barrier, which  
 628 connects the aluminium grains. The difference from the experiment  
 629 by Kuzmin et al.<sup>108</sup>, as well as in the earlier work of Fazio et al.<sup>8</sup> is  
 630 that the aluminium islands in granular aluminum are very small.  
 631 The size of the grains may lead to a situation in which energy level

spacing exceeds the pairing gap, which may be important for the  
 understanding of the results reported by Lévy-Bertrand et al.<sup>112</sup>.

The experimental work described in the previous paragraphs  
 makes clear that an ideal superinductor does require thought-  
 ful experimental work. At the same time, the research on the QBS  
 has uncovered the various ways in which superconductors with  
 high normal state resistivity lose their superconducting proper-  
 ties. These pathways take into account the nature of the coupling  
 of the superconducting phases, as well as the possibility of local-  
 ized pairs and the pairing strength. With the ultimate goal of lossless  
 inductors the materials requirements have been discussed in recent  
 publications by Feigel'man and Ioffe<sup>115,116</sup>. Many challenges towards  
 a usable superinductor are ahead of us and will need to be com-  
 pared with the use of arrays of tunnel junctions aiming for the same  
 functionality<sup>108</sup>.

## Open problems and conclusions

The key challenge for understanding superconductivity is that a  
 macroscopic quantum state emerges from or gets destroyed by  
 microscopic quantum properties. In this Review we have identi-  
 fied several pathways for this process, all of which may occur in real  
 materials. Since our interest is not so much in one specific model  
 system, nor in just plausible interpretations of experiments, but in  
 a description of real world materials, the additional challenge is to  
 identify which pathway is most likely applicable to a specific mater-  
 ial system, while at the same time acknowledging that perhaps  
 there are other pathways that have not been identified or properly  
 solved yet.

To close, we would like to highlight several experimental obser-  
 vations have not yet been understood:

- For homogeneously disordered superconductors, assessing an effective Coulomb interaction is conceptually difficult: The absence of grain boundaries makes it difficult to define an equivalent capacitance that determines charging effects in tunnel junctions and the ensuing phase fluctuations. Therefore, addressing quantum phase fluctuations in superconductors on the basis of Josephson junction models remains purely qualitative and should not disguise the fact that exact role of Coulomb interaction on phase fluctuations in disordered superconductors is an open question.
- In the vicinity of a SMT, a strange metal state is frequently observed<sup>9</sup>. Do these observations indicate the existence of an intrinsic equilibrium quantum state, which may result from the intricate interplay between Cooper pairing, Coulomb repulsion and Anderson localization? Or are these observations in need of a careful reexamination of the experimental conditions under which the data have been taken, because of a possible coupling to the non-equilibrium environment?
- The experimentally observed high sensitivity<sup>10,11</sup> to radio-wave interference, as known for Josephson junctions with either an insulating or normal metal weak link<sup>70</sup>, calls for an analysis of the effect of microwaves on the study of superconducting materials, which are expected to be spatially inhomogeneous. Both the common Josephson response due to a local voltage difference that affects the local phase differences and the non-equilibrium effects that change the Josephson coupling should be considered.
- For the magnetic-field-driven QBS in moderately disordered materials, the nature of the strongly pinned vortex glass in the  $T = 0$  limit is still unclear<sup>55</sup>. The theoretical problem is to describe a vortex glass with a macroscopic superfluid density  $\rho_s$ . In the strong disorder limit, a combined account of the localization of preformed pairs and Coulomb interaction is still to be developed.
- Can one avoid the low-energy collective modes in pseudogap superconductors? This is an issue of practical importance for the

development of various quantum circuits where a high kinetic inductance proportional to  $1/\rho_s$ , should be combined with an absence of dissipation at frequencies in the sub-gigahertz range.

- The giant magnetoresistance peak terminating superconductivity in some materials (a:InO, refs. <sup>117–119</sup>; TiN, ref. <sup>120</sup>; nano-patterned a-Bi, refs. <sup>121,122</sup>; proximitized graphene, ref. <sup>22</sup>) continues to defy understanding. New experimental approaches must be employed to probe this insulating state beyond transport measurements that have proven to be limited by non-equilibrium effects<sup>123</sup>.
- On the insulating side of a SIT we may encounter a many-body localized state, with extremely weak electron–phonon coupling<sup>124</sup> and conductivity vanishing at some nonzero temperature<sup>125</sup>.
- Lastly, understanding which microscopic parameters and phenomena define the metallic-like or insulating nature of the ground state terminating superconductivity for given material, that is, SMT versus SIT, remains a major question.

Future research is expected to focus on the interaction between the three themes addressed in this review: theory, experiments and applications. Experiments unavoidably will have to focus on model systems, which allow them to evaluate identified theoretical pathways. Applications have the virtue of providing large amounts of experimental data, assuming they have been taken under relevant experimental circumstances and with a good knowledge of the details of how the system interacts with its environment. From the latter point of view the increased use of strongly disordered superconducting materials for astronomical instrumentation and quantum computation holds the potential of providing data that are significant for evaluation based on the available theoretical models.

Finally, we expect that the subject of quantum breakdown of superconductivity will benefit from the increasing availability of gateable 2D superconducting systems<sup>126–128</sup> that constitute well-defined atomically uniform model systems in which specific pathways could be tested in much detail.

Received: 18 October 2019; Accepted: 9 April 2020;

## References

- Sondhi, S. L., Girvin, S. M., Carini, J. P. & Shahar, D. Continuous quantum phase transitions. *Rev. Mod. Phys.* **69**, 315–333 (1997).
- Goldman, A. M. & Markovic, N. Superconductor-insulator transitions in the two-dimensional limit. *Phys. Today* **51**, 39–44 (1998).
- Larkin, A. I. Superconductor-insulator transitions in films and bulk materials. *Ann. Phys.* **8**, 785–794 (1999).
- Finkelstein, A. M. Superconducting transition temperature in amorphous films. *JETP Lett.* **45**, 46–49 (1987).
- Finkelstein, A. M. Suppression of superconductivity in homogeneously disordered systems. *Physica B* **197**, 636–648 (1994).
- Fisher, M. P. A. Quantum phase transitions in disordered two-dimensional superconductors. *Phys. Rev. Lett.* **65**, 923–926 (1990).
- Larkin, A. & Varlamov, A. *Theory of fluctuations in superconductors* (Clarendon, 2005).
- Fazio, R. & Van der Zant, H. S. J. Quantum phase transitions and vortex dynamics in superconducting networks. *Phys. Rep.* **355**, 235–334 (2001).
- Kapitulnik, A., Kivelson, S. & Spivak, B. Z. Anomalous metals: failed superconductors. *Rev. Mod. Phys.* **91**, 011002 (2019).
- Tamir, I. et al. Sensitivity of the superconducting state in thin films. *Sci. Adv.* **5** (2019).
- Dutta, S. et al. Extreme sensitivity of the vortex state in *a*-MoGe films to radio-frequency electromagnetic perturbation. *Phys. Rev. B* **100**, 214518 (2019).
- Emery, V. J. & Kivelson, S. A. Importance of phase fluctuations in superconductors with small superfluid density. *Nature* **374**, 434–437 (1995).
- Altshuler, B. L. & Aronov, A. G. *Electron-Electron Interaction in Disordered Conductors* (eds Efros, A. L. & Pollak, M.) (Elsevier, 1985).
- Hebard, A. F. & Paalanen, M. A. Magnetic-field-tuned superconductor-insulator transition in two-dimensional films. *Phys. Rev. Lett.* **65**, 927–930 (1990).

- Haviland, D. B., Liu, Y. & Goldman, A. M. Onset of superconductivity in the two-dimensional limit. *Phys. Rev. Lett.* **62**, 2180–2183 (1989).
- Steiner, M. A., Breznay, N. P. & Kapitulnik, A. Approach to a superconductor-to-bose-insulator transition in disordered films. *Phys. Rev. B* **77**, 212501 (2008).
- Gantmakher, V. F. & Dolgoplov, V. T. Superconductor-insulator quantum phase transition. *Phys. Usp.* **53**, 1–49 (2010).
- Lin, Y.-H., Nelson, J. & Goldman, A. M. Superconductivity of very thin films: the superconductor-insulator transition. *Physica C* **514**, 130–141 (2015).
- Biscaras, J. et al. Multiple quantum criticality in a two-dimensional superconductor. *Nat. Mater.* **12**, 542–548 (2013).
- Sambandamurthy, G. et al. Power law resistivity behavior in 2D superconductors across the magnetic field-tuned superconductor-insulator transition. *Europhys. Lett.* **75**, 611–617 (2006).
- Bollinger, A. T. et al. Superconductor-insulator transition in  $\text{La}_{2-x}\text{CuO}_4$  at the pair quantum resistance. *Nature* **472**, 458–460 (2011).
- Allain, A., Han, Z. & Bouchiat, V. Electrical control of the superconducting-to-insulating transition in graphene-metal hybrids. *Nat. Mater.* **11**, 590–594 (2012).
- Baturina, T. I., Mironov, A. Y., Vinokur, V. M., Baklanov, M. R. & Strunk, C. Localized superconductivity in the quantum-critical region of the disorder-driven superconductor-insulator transition in TiN thin films. *Phys. Rev. Lett.* **99**, 257003 (2007).
- Maekawa, S. & Fukuyama, H. Localization effects in two-dimensional superconductors. *J. Phys. Soc. Japan* **51**, 1380–1385 (1982).
- Takagi, H. & Kuroda, Y. Anderson localization and superconducting transition temperature in two-dimensional systems. *Solid State Commun.* **41**, 643–648 (1982).
- Sacépé, B. et al. Disorder-induced inhomogeneities of the superconducting state close to the superconductor-insulator transition. *Phys. Rev. Lett.* **101**, 157006 (2008).
- Sacépé, B. et al. Pseudogap in a thin film of a conventional superconductor. *Nat. Commun.* **1**, 140 (2010).
- Mondal, M. et al. Phase fluctuations in a strongly disordered *s*-wave NbN superconductor close to the metal-insulator transition. *Phys. Rev. Lett.* **106**, 047001 (2011).
- Sacépé, B. et al. Localization of preformed cooper pairs in disordered superconductors. *Nat. Phys.* **7**, 239–244 (2011).
- Chand, M. et al. Phase diagram of the strongly disordered *s*-wave superconductor NbN close to the metal-insulator transition. *Phys. Rev. B* **85**, 014508 (2012).
- Sherman, D., Kopnov, G., Shahar, D. & Frydman, A. Measurement of a superconducting energy gap in a homogeneously amorphous insulator. *Phys. Rev. Lett.* **108**, 177006 (2012).
- Noat, Y. et al. Unconventional superconductivity in ultrathin superconducting NbN films studied by scanning tunneling spectroscopy. *Phys. Rev. B* **88**, 014503 (2013).
- Ganguly, R. et al. Magnetic field induced emergent inhomogeneity in a superconducting film with weak and homogeneous disorder. *Phys. Rev. B* **96**, 054509 (2017).
- Zhao, K. et al. Disorder-induced multifractal superconductivity in monolayer niobium dichalcogenides. *Nat. Phys.* **15**, 904–910 (2019).
- Larkin, A. I. & Ovchinnikov, Y. N. Density of states in inhomogeneous superconductors. *Sov. Phys. JETP* **34**, 1144–1150 (1972).
- Ghosal, A., Randeria, M. & Trivedi, N. Role of spatial amplitude fluctuations in highly disordered *s*-Wave superconductors. *Phys. Rev. Lett.* **81**, 3940–3943 (1998).
- Meyer, J. S. & Simons, B. D. Gap fluctuations in inhomogeneous superconductors. *Phys. Rev. B* **64**, 134516 (2001).
- Ghosal, A., Randeria, M. & Trivedi, N. Inhomogeneous pairing in highly disordered *s*-wave superconductors. *Phys. Rev. B* **65**, 014501 (2001).
- Skvortsov, M. A. & Feigel'man, M. V. Superconductivity in disordered thin films: giant mesoscopic fluctuations. *Phys. Rev. Lett.* **95**, 057002 (2005).
- Dubi, Y., Meir, Y. & Avishai, Y. Nature of the superconductor-insulator transition in disordered superconductors. *Nature* **449**, 876–880 (2007).
- Bouadim, K., Loh, Y. L., Randeria, M. & Trivedi, N. Single- and two-particle energy gaps across the disorder-driven superconductor-insulator transition. *Nat. Phys.* **7**, 884–889 (2011).
- Feigel'man, M. V. & Skvortsov, M. A. Universal Broadening of the Bardeen-Cooper-Schrieffer Coherence Peak of Disordered Superconducting Films. *Phys. Rev. Lett.* **109**, 147002 (2012).
- Lemarié, G. et al. Universal scaling of the order-parameter distribution in strongly disordered superconductors. *Phys. Rev. B* **87**, 184509 (2013).
- Stosiek, M., Lang, B. & Evers, F. Self-consistent-field ensembles of disordered Hamiltonians: efficient solver and application to superconducting films. Preprint at <https://arxiv.org/abs/1903.10395v2> (2019).

- 698 45. Ma, M. & Lee, P. A. Localized superconductors. *Phys. Rev. B* **32**,  
699 5658–5667 (1985).
- 700 46. Kapitulnik, A. & Kotliar, G. Anderson localization and the theory of dirty  
701 superconductors. *Phys. Rev. Lett.* **54**, 473–476 (1985).
- 702 47. Kotliar, G. & Kapitulnik, A. Anderson localization and the theory of dirty  
703 superconductors. II. *Phys. Rev. B* **33**, 3146–3157 (1986).
- 704 48. Feigelman, M. V., Ioffe, L. B., Kravtsov, V. E. & Yuzbashyan, E. A.  
705 Eigenfunction fractality and pseudogap state near the  
706 superconductor-insulator transition. *Phys. Rev. Lett.* **98**, 027001 (2007).
- 707 49. Feigelman, M. V., Ioffe, L. B., Kravtsov, V. E. & Cuevas, E. Fractal  
708 superconductivity near localization threshold. *Ann. Phys.* **325**,  
709 1390–1478 (2010).
- 710 50. Anderson, P. W. Possible consequences of negative U centers in amorphous  
711 materials. *J. Phys. Coll.* **37**, 339–342 (1976).
- 712 51. Cuevas, E. & Kravtsov, V. E. Two-eigenfunction correlation in a multifractal  
713 metal and insulator. *Phys. Rev. B* **76**, 235119 (2007).
- 714 52. Evers, F. & Mirlin, A. D. Anderson transitions. *Rev. Mod. Phys.* **80**,  
715 1355–1417 (2008).
- 716 53. Burmistrov, I. S., Gornyi, I. V. & Mirlin, A. D. Enhancement of the critical  
717 temperature of superconductors by Anderson localization. *Phys. Rev. Lett.*  
718 **108**, 017002 (2012).
- 719 54. Burmistrov, I. S., Gornyi, I. V. & Mirlin, A. D. Superconductor-insulator  
720 transitions: phase diagram and magnetoresistance. *Phys. Rev. B* **92**,  
721 014506 (2015).
- 722 55. Sacépé, B. et al. Low-temperature anomaly in disordered superconductors  
723 near  $B_{c2}$  as a vortex-glass property. *Nat. Phys.* **15**, 48–53 (2019).
- 724 56. Skvortsov, M. A., Larkin, A. I. & Feigelman, M. V. Dephasing in disordered  
725 metals with superconductive grains. *Phys. Rev. Lett.* **92**, 247002 (2004).
- 726 57. Spivak, B. & Zhou, F. Mesoscopic effects in disordered superconductors  
727 near  $h_{c2}$ . *Phys. Rev. Lett.* **74**, 2800–2803 (1995).
- 728 58. Tikhonov, K. S. & Feigelman, M. V. Strange metal state near quantum  
729 superconductor-metal transition in thin films. Preprint at <https://arxiv.org/abs/2002.08107> (2020).
- 730 59. Kirkpatrick, T. R. & Belitz, D. Metal-superconductor transition  
731 at zero temperature: a case of unusual scaling. *Phys. Rev. Lett.* **79**,  
732 3042–3045 (1997).
- 733 60. Frydman, A. The superconductor insulator transition in systems of  
734 ultrasmall grains. *Physica C* **391**, 189–195 (2003).
- 735 61. Carbillet, C. et al. Confinement of superconducting fluctuations due to  
736 emergent electronic inhomogeneities. *Phys. Rev. B* **93**, 144509 (2016).
- 737 62. Carbillet, C. et al. Spatial cross-correlations between local electron-electron  
738 interaction effects and local superconducting energy gap in  
739 moderately-disordered NbN ultrathin films. Preprint at: <https://arxiv.org/abs/1903.01802> (2019).
- 740 63. Altshuler, B. L., Aronov, A. G. & Lee, P. A. Interaction effects in disordered  
741 Fermi Systems in two dimensions. *Phys. Rev. Lett.* **44**, 1288–1291 (1980).
- 742 64. Galitski, V. M. & Larkin, A. I. Disorder and Quantum Fluctuations in  
743 Superconducting Films in Strong Magnetic Fields. *Phys. Rev. Lett.* **87**,  
744 087001 (2001).
- 745 65. Lotnyk, D. Suppression of the superconductivity in ultrathin amorphous  
746  $\text{Mo}_x\text{Ge}_{22}$  films observed by STM. *Low Temp. Phys.* **43**, 919–923 (2017).
- 747 66. Dubouchet, T. et al. Collective energy gap of preformed Cooper pairs in  
748 disordered superconductors. *Nat. Phys.* **15**, 233–236 (2019).
- 749 67. Szabó, P. et al. Fermionic scenario for the destruction of superconductivity  
750 in ultrathin MoC films evidenced by STM measurements. *Phys. Rev. B* **93**,  
751 014505 (2016).
- 752 68. Skvortsov, M. A. & Feigelman, M. V. to be found. *Z. Exp. Theor. Fiz.* **144**,  
753 560 (2013).
- 754 69. le Sueur, H. & Joyez, P. Room-temperature tunnel current amplifier and  
755 experimental setup for high resolution electronic spectroscopy in  
756 millikelvin scanning tunneling microscope experiments. *Rev. Sci. Instrum.*  
757 **77**, 123701 (2006).
- 758 70. Martinis, J. M. & Nahum, M. Effect of environmental noise on the accuracy  
759 of Coulomb-blockade devices. *Phys. Rev. B* **48**, 18316–18319 (1993).
- 760 71. Fischer, Ø., Kugler, M., Maggio-Aprile, I., Berthod, C. & Renner, C.  
761 Scanning tunneling spectroscopy of high-temperature superconductors. *Rev.*  
762 *Mod. Phys.* **79**, 353–419 (2007).
- 763 72. Varlamov, A. A. & Dorin, V. V. Fluctuation resistance of Josephson  
764 junctions. *Sov. Phys. JETP* **57**, 1089–1096 (1983).
- 765 73. Mandal, S. Destruction of superconductivity through phase fluctuations in  
766 ultrathin a-moqe films. Preprint at <https://arxiv.org/abs/2003.12398> (2020).
- 767 74. Levitov, L. S. & Shytov, A. V. Semiclassical theory of the Coulomb anomaly.  
768 *JETP Letters* **66**, 214 (1997).
- 769 75. Deutscher, G. Coherence and single-particle excitations in the  
770 high-temperature superconductors. *Nature* **397**, 410–412 (1999).
- 771 76. Deutscher, G. Andreev–Saint-James reflections: a probe of cuprate  
772 superconductors. *Rev. Mod. Phys.* **77**, 109–135 (2005).
- 773 77. Matveev, K. A. & Larkin, A. I. Parity effect in ground state energies of  
774 ultrasmall superconducting grains. *Phys. Rev. Lett.* **78**, 3749–3752 (1997).
- 775 78. Shahar, D. & Ovadyahu, Z. Superconductivity near the mobility edge.  
776 *Phys. Rev. B* **46**, 10917–10922 (1992).
- 777 79. Gantmakher, V. F., Golubkov, M. V., Lok, J. G. S. & Geim, A. K. Giant  
778 negative magnetoresistance of semi-insulating amorphous indium oxide  
779 films in strong magnetic fields. *JETP* **82**, 951–958 (1996).
- 780 80. Mott, N. F. & Davis, E. A. *Electronic Properties in Non-Crystalline Materials*  
(Clarendon, 1971).
- 781 81. Anderson, P. W. Random-phase approximation in the theory of  
782 superconductivity. *Phys. Rev.* **112**, 1900–1916 (1958).
- 783 82. Feigelman, M. V., Ioffe, L. B. & Mézard, M. Superconductor-insulator  
784 transition and energy localization. *Phys. Rev. B* **82**, 184534 (2010).
- 785 83. Carpentier, D. & Le Doussal, P. Topological transitions and freezing in XY  
786 models and Coulomb gases with quenched disorder: renormalization via  
787 traveling waves. *Nucl. Phys. B* **588**, 565–629 (1995).
- 788 84. Kowal, D. & Ovadyahu, Z. Scale dependent superconductor-insulator  
789 transition. *Physica C* **468**, 322–325 (2008).
- 790 85. Spathis, P., Aubin, H., Pourret, A. & Behnia, K. Nernst effect in the  
791 phase-fluctuating superconductor  $\text{InO}_x$ . *Europhys. Lett.* **83**, 57005 (2008).
- 792 86. Pourret, A., Spathis, P., Aubin, H. & Behnia, K. Nernst effect as a probe of  
793 superconducting fluctuations in disordered thin films. *New J. Phys.* **11**,  
794 055071 (2009).
- 795 87. Refael, G. & Altman, E. Strong disorder renormalization group primer and  
796 the superfluid-insulator transition. *Compt. Rend. Phys.* **14**, 725–739 (2013).
- 797 88. Igloi, F. & Monthus, C. Strong disorder RG approach - a short review of  
798 recent developments. *Eur. Phys. J. B* **91**, 290 (2014).
- 799 89. Fisher, D. S. Critical behavior of random transverse-field Ising spin chains.  
800 *Phys. Rev. B* **51**, 6411–6461 (1995).
- 801 90. Abraham, D. W., Lobb, C. J., Tinkham, M. & Klapwijk, T. M. Resistive  
802 transition in two-dimensional arrays of superconducting weak links.  
803 *Phys. Rev. B* **26**, 5268–5271 (1982).
- 804 91. Eley, S., Gopalakrishnan, S., Goldbart, P. M. & Mason, N. Approaching  
805 zero-temperature metallic states in mesoscopic superconductor-normal-  
806 superconductor arrays. *Nat. Phys.* **8**, 59–62 (2012).
- 807 92. Han, Z. et al. Collapse of superconductivity in a hybrid tin-graphene  
808 Josephson junction array. *Nat. Phys.* **10**, 380–386 (2014).
- 809 93. Bottcher, C. G. L. et al. Superconducting, insulating and anomalous metallic  
810 regimes in a gated two-dimensional semiconductor-superconductor array.  
811 *Nat. Phys.* **14**, 1138–1144 (2018).
- 812 94. Kjaergaard, M. et al. Transparent Semiconductor-Superconductor Interface  
813 and Induced Gap in an Epitaxial Heterostructure Josephson Junction. *Phys.*  
814 *Rev. Appl.* **7**, 034029 (2017).
- 815 95. Martinis, J. M., Devoret, M. H. & Clarke, J. Experimental tests for the  
816 quantum behavior of a macroscopic degree of freedom: the phase difference  
817 across a Josephson junction. *Phys. Rev. B* **35**, 4682–4698 (1987).
- 818 96. Barends, R. et al. Minimizing quasiparticle generation from stray  
819 infrared light in superconducting quantum circuits. *Appl. Phys. Lett.* **99**,  
820 113507 (2011).
- 821 97. Kang, J. et al. On-chip intercalated-graphene inductors for next-generation  
822 radio frequency electronics. *Nat. Electron.* **1**, 46–51 (2018).
- 823 98. Douçot, B. & Lofe, L. B. Physical implementation of protected qubits. *Rep.*  
824 *Prog. Phys.* **75**, 072001 (2012).
- 825 99. Brooks, P., Kitaev, A. & Preskill, J. Protected gates for superconducting  
826 qubits. *Phys. Rev. A* **87**, 052306 (2013).
- 827 100. Groszkowski, P. et al. Coherence properties of the  $0-\pi$  qubit. *New J. Phys.*  
828 **20**, 043053 (2018).
- 829 101. Smith, W. C., Kou, A., Xiao, X., Vool, U. & Devoret, M. H.  
830 Superconducting circuit protected by two-Cooper-pair tunneling.  
831 *npj Quant. Inf.* **6**, 8 (2020).
- 832 102. Mooij, J. E. & Harmans, C. J. P. M. Phase-slip flux qubits. *New J. Phys.* **7**,  
833 219–219 (2005).
- 834 103. Mooij, J. E. & Nazarov, Y. V. Superconducting nanowires as quantum  
835 phase-slip junctions. *Nat. Phys.* **2**, 169–172 (2006).
- 836 104. Astafiev, O. V. et al. Coherent quantum phase slip. *Nature* **484**,  
837 355–358 (2012).
- 838 105. Peltonen, J. T. et al. Coherent dynamics and decoherence in a  
839 superconducting weak link. *Phys. Rev. B* **94**, 180508 (2016).
- 840 106. Peltonen, J. T. et al. Hybrid rf SQUID qubit based on high kinetic  
841 inductance. *Sci. Rep.* **8**, 10033 (2018).
- 842 107. de Graaf, S. E., Shaikhaidarov, R., Lindstrom, T., Tzalenchuk, A. Y. &  
843 Astafiev, O. V. Charge control of blockade of Cooper pair tunneling in  
844 highly disordered TiN nanowires in an inductive environment. *Phys. Rev. B*  
845 **99**, 205115 (2019).
- 846 108. Kuzmin, R. et al. Quantum electrodynamics of a superconductor-insulator  
847 phase transition. *Nat. Phys.* **15**, 930–934 (2019).
- 848 109. Maleeva, N. et al. Circuit quantum electrodynamics of granular aluminum  
849 resonators. *Nat. Commun.* **9**, 3889 (2018).
- 850 110. Grünhaupt, L. et al. Loss mechanisms and quasiparticle dynamics in  
851 superconducting microwave resonators made of thin-film granular  
852 aluminum. *Phys. Rev. Lett.* **121**, 117001 (2018).

- 764 111. Grünhaupt, L. et al. Granular aluminium as a superconducting  
765 material for high-impedance quantum circuits. *Nat. Mater.* **18**,  
766 816–819 (2019).  
767 112. Levy-Bertrand, F. et al. Electrodynamics of granular aluminum from  
768 superconductor to insulator: Observation of collective superconducting  
769 modes. *Phys. Rev. B* **99**, 094506 (2019).  
770 113. Wenyuan, Z. et al. Microresonators Fabricated from High-Kinetic-  
771 Inductance Aluminum Films. *Phys. Rev. Appl.* **11**, 011003 (2019).  
772 114. Kamenov, P. et al. Granular aluminum meandered superinductors for  
773 quantum circuits. Preprint at <https://arxiv.org/1910.00996v1> (2019).  
774 115. Feigel'man, M. V. & Ioffe, L. B. Superfluid density of a pseudogapped  
775 superconductor near the superconductor-insulator transition. *Phys. Rev. B*  
776 **92**, 100509 (2015).  
777 116. Feigel'man, M. V. & Ioffe, L. B. Microwave properties of superconductors  
778 close to the superconductor-insulator transition. *Phys. Rev. Lett.* **120**,  
779 037004 (2018).  
780 117. Gantmakher, V. F., Golubkov, M. V., Dolgoplov, V. T., Shashkin, A. &  
781 Tsydynzhapov, G. E. Observation of the parallel-magnetic-field-induced  
782 superconductor-insulator transition in thin amorphous InO films.  
783 *JETP Lett.* **71**, 473–476 (2000).  
784 118. Sambandamurthy, G., Engel, L. W., Johansson, A. & Shahar, D.  
785 Superconductivity-related insulating behavior. *Phys. Rev. Lett.* **92**,  
786 107005 (2004).  
787 119. Steiner, M. & Kapitulnik, A. Superconductivity in the insulating phase  
788 above the field-tuned superconductor-insulator transition in disordered  
789 indium oxide films. *Physica C* **422**, 16–26 (2005).  
790 120. Baturina, T. I., Strunk, C., Baklanov, M. R. & Satta, A. Quantum metallicity  
791 on the high-field side of the superconductor-insulator transition. *Phys. Rev.*  
792 *Lett.* **98**, 127003 (2007).  
793 121. Stewart, M. D., Yin, A., Xu, J. M. & Valles, J. M. Superconducting pair  
794 correlations in an amorphous insulating nanohoneycomb film. *Science* **318**,  
795 5854 (2007).  
796 122. Nguyen, H. Q. et al. Observation of giant positive magnetoresistance in a  
797 Cooper pair insulator. *Phys. Rev. Lett.* **103**, 157001 (2009).  
798 123. Doron, A. Instability of insulators near quantum phase transitions.  
799 *Phys. Rev. Lett.* **119**, 247001 (2017).  
800 124. Ovadia, M., Sacépé, B. & Shahar, D. Electron-phonon decoupling in  
801 disordered insulators. *Phys. Rev. Lett.* **102**, 176802 (2009).  
802 125. Ovadia, M. et al. Evidence for a finite-temperature insulator. *Sci. Rep.* **5**,  
803 13503 (2015).  
804  
805  
806  
807  
808  
809  
810  
811  
812  
813  
814  
815  
816  
817  
818  
819  
820  
821
126. Caviglia, A. D. et al. Electric field control of the LaAlO<sub>3</sub>/SrTiO<sub>3</sub> interface  
ground state. *Nature* **456**, 624–627 (2008).  
127. Tsen, A. W. et al. Nature of the quantum metal in a two-dimensional  
crystalline superconductor. *Nat. Phys.* **12**, 208–212 (2016).  
128. Cao, Y. et al. Unconventional superconductivity in magic-angle graphene  
superlattices. *Nature* **556**, 43–50 (2018).  
129. Berezinskii, V. L. Destruction of long-range order in one-dimensional and  
two-dimensional systems possessing a continuous symmetry group. II.  
Quantum systems. *Sov. Phys. JETP Lett.* **34**, 610 (1972).  
130. Kosterlitz, J. M. & Thouless, D. J. Ordering, metastability and phase  
transitions in two-dimensional systems. *J. Phys. C* **6**, 1181 (1973).  
131. Strongin, M., Thompson, R. S., Kammerer, O. F. & Crow, J. E. Destruction  
of superconductivity in disordered near-monolayer films. *Phys. Rev. B* **1**,  
1078–1091 (1970).

## Acknowledgements

We thank the participants of the workshop on The Challenge of 2-Dimensional Superconductivity (8–12 July 2019, Lorentz Center, University of Leiden) for providing us with up-to-date insight into the various viewpoints on the subject. B.S. has received funding from the European Research Council (ERC) under the H2020 programme (grant no. 637815) and from the French National Research Agency (ANR grant CP-Insulator). M.F. is supported by a Skoltech NGP grant and by the RAS program Advanced Problems in Low Temperature Physics. T.M.K. is supported by a grant from the Russian Science Foundation (no. 17-72-30036) and by the Würzburg-Dresden Center of Excellence on Complexity and Topology in Quantum Matter (CT.QMAT).

## Competing interests

The authors declare no competing interests.

## Additional information

Correspondence should be addressed to B.S.

Peer review information *Nature Physics* thanks Hermann Suderow and the other, anonymous, reviewer(s) for their contribution to the peer review of this work.

Reprints and permissions information is available at [www.nature.com/reprints](http://www.nature.com/reprints).

Publisher's note Springer Nature remains neutral with regard to jurisdictional claims in published maps and institutional affiliations.

© Springer Nature Limited 2020

# QUERY FORM

|                       |                        |
|-----------------------|------------------------|
| <b>Nature Physics</b> |                        |
| <b>Manuscript ID</b>  | [Art. Id: 905]         |
| <b>Author</b>         | <b>Benjamin Sacépé</b> |

**AUTHOR:**

The following queries have arisen during the editing of your manuscript. Please answer by making the requisite corrections directly in the e-proofing tool rather than marking them up on the PDF. This will ensure that your corrections are incorporated accurately and that your paper is published as quickly as possible.

| <i>Query No.</i> | <i>Nature of Query</i>   |
|------------------|--|
| Q1:              | Please check your article carefully, coordinate with any co-authors and enter all final edits clearly in the eproof, remembering to save frequently. Once corrections are submitted, we cannot routinely make further changes to the article.  |
| Q2:              | Note that the eproof should be amended in only one browser window at any one time; otherwise changes will be overwritten.  |
| Q3:              | Author surnames have been highlighted. Please check these carefully and adjust if the first name or surname is marked up incorrectly. Note that changes here will affect indexing of your article in public repositories such as PubMed. Also, carefully check the spelling and numbering of all author names and affiliations, and the corresponding email address(es). |
| Q4:              | In the sentence beginning ‘We restrict use of’, could ‘it’ be replaced, for clarity? Perhaps this could be ‘if the superconductor transitions into a metal-like state’, or similar?  |
| Q5:              | Journal style does not permit multi-part headings, and so ‘Quantum Breakdown of Superconductivity:’ has been removed from the beginning of the heading ‘Amplitude- versus phase-driven transition’. Please confirm that this is okay and that the new heading has been edited correctly.   |
| Q6:              | In the sentence beginning ‘In this case’, single quotes were added around ‘bad’ to indicate that this means ‘a so-called bad metal’. Is this okay/appropriate?   |
| Q7:              | Fig. 2b: $\phi$ is used in the caption, but $\psi$ is in the figure itself. Is this correct, or should one be changed? Fig. 2c: Please define x and y.   |
| Q8:              | In the sentence beginning ‘Andreev reflections’, please define the superscript C.  |
| Q9:              | In the sentence beginning ‘However, in low’, ‘tenths of meV’ was changed to ‘on the order of 0.1 meV’, is this okay?   |
| Q10:             | In the sentence beginning ‘We assume, going’, what does ‘Section IV’ refer to? If this is an earlier section of this paper, could this be replaced by ‘above’, or the name of the section?   |
| Q11:             | In the sentence beginning ‘When such a bulk disordered system’, what is meant by ‘with a tendency to electron pairing’? Could this be reworded as ‘with a tendency to undergo electron pairing’ or similar, for clarity?   |
| Q12:             | In the sentence beginning ‘The hopping terms’, please define h.c. Is this the Hermitian conjugate?   |
| Q13:             | In the sentence beginning ‘The total number of disks’, please confirm that the units are correct; they were changed  |

